OPTIMIZATION OF SOLID FUEL PRODUCTION BY CO-HYDROTHERMAL CARBONIZATION OF POLYVINYL CHLORIDE AND PONTEDERIA CRASSIPES

By

Solomon Asare

(BSc. Agricultural Engineering)

A thesis submitted to The Department of Agricultural and Biosystems Engineering, Kwame Nkrumah University of Science and Technology, Kumasi in partial fulfilment of the requirement for the degree of

MASTER OF PHILOSOPHY IN BIOENGINEERING

July 2023

DECLARATION

I hereby declare that this submission is my work, and that to the best of my knowledge and belief, it contains no material previously published or written by another person nor material which to a substantial extent has been accepted for the award of any other degree or diploma at Kwame Nkrumah University of Science and Technology or any other institution, except where due acknowledgement is made in the thesis.

Solomon Asare (PG5764020)	……	……
Name of Student	Signature	Date

Certified by

Prof. Francis Kemausuor	……	……
Name of Supervisor	Signature	Date

Certified by

Prof. Ahmad Addo	……	……
Name of Supervisor	Signature	Date

Certified by

Prof. Francis Kemausuor	……	……
Head of Department	Signature	Date

ABSTRACT

The chlorine content of Polyvinyl chloride (PVC) in municipal waste creates a major challenge in its disposal. Water hyacinth (WH), an invasive plant, disrupts aquatic life and impedes the movement of vessels on water bodies that they colonize. These two materials, PVC and WH however have high caloric value making them suitable to be used as a source of fuel. Hydrothermal carbonization (HTC), a method for producing solid fuel has been identified as a safe medium to remove chlorine from PVC. In this work, PVC, and WH were subjected to Co-HTC using water as the solvent. Response Surface Methodology (RSM) was used to optimize the hydrochar produced by varying the temperatures, residence time, and mixing ratios. 5 g of the feedstock was subjected to Co-HTC at temperatures 200 ℃, 230 ℃, and 260 ℃; residence time of 60 minutes, 90 minutes, and 120 minutes; and mixing ratio of PVC/WH 1:1 to 1:3. The result showed that increasing the temperature and resident time increased the dechlorination efficiency (DE) of the PVC with the highest DE at 94.3%. The mixing ratio had a minimal effect on the output variables. Increasing temperatures and residence time reduced the mass yield of hydrochar but increased their corresponding High Heating Values (HHV). The highest hydrochar yield, 70.33%, occurred at 200 ℃, the highest DE of 94.39% occurred at 260 ℃, and the highest HHV, 32.34 MJ/Kg occurred at 260 ℃. FTIR microscopy, TGA analysers, and Van Krevelen diagrams were used in analysing the thermal properties of the fuel produced. The optimal conditions predicted from the data using the RSM are temperature, 230 ℃, residence time, 86 minutes, and mixing ratio of 0.33. These parameters were used for the confirmation and validation and the HHV obtained was 27.32 MJ/Kg. The HHV is close to that of coal, implying that hydrochar produced from PVC and WH feedstocks can be a good source of fuel for domestic and industrial usage.

TABLE OF CONTENTS

LIST OF FIGURES

ACKNOWLEDGEMENTS

My foremost thanks go to the Almighty God for granting me the wisdom, strength, and protection for me to complete this work.

My appreciation goes to the German Ministry of Science and Education through the Brew Hammond Energy Center for funding this project which was under the theme "Hybrid Waste to Energy as a Sustainable Solution for Ghana. I am very grateful to my supervisors: Prof. Francis Kemausuor and Mr. Michael Commeh for the guidance and assistance they provided me. It was indispensable. I am also grateful to Prof. Ahmad Addo for his invaluable support.

Finally, I would like to appreciate Mr. Augustine Sackey and Ms. Sarah Oppong Nketiah for being part of the editorial team. I appreciate Mrs. Rebecca Adomeh Mawunyo, Ms. Rebecca Asare, and Mrs. Comfort Asare for supporting me throughout the period. May God bless you all

CHAPTER ONE

INTRODUCTION

1.1 Background of Study

Due to the rising population of the world, coupled with the increasing energy demands and concerns about global warming, new alternative energy options with a low carbon footprint are being sought. Furthermore, the grave threat of global warming caused by greenhouse gases, as well as the depletion of commercially available conventional fossil fuels, restricts their use. To reduce our dependency on fossil fuels, there is the need to focus attention on the conversion of waste into a more useful form such as energy, alternative fuel, and nutrient. The global waste generation reached 3.4 x 10^9 metric tonnes in 2020, with only a 20% recycling rate (World Bank data, 2020). Municipal plastic waste (MPW) generation has been gradually increasing at a rate of 5% per year, but MPW recycling is only at 3% per year; the rest of MPW is either disposed of by landfill or incinerated (Zhao *et a*l., 2020). Due to their versatility, plastics are widely used in automobiles, electronics, and construction. A popular plastic, Polyvinyl Chloride (PVC) shares a major percentage in construction followed by Polyethylene (PE) and Polyethylene Terephthalate (PET). This has resulted in the increase of chlorine content in municipal solid waste (MSW). Incineration of these waste which contain chlorine results in its subsequent release into the atmosphere, posing dander to the environment. Hydrothermal carbonization, a thermochemical process, can absorb the chlorine in waste into its process water during the reaction, thereby preventing its release into the atmosphere. Biomass and PVC meet all of the criteria for renewable and carbon-neutral energy sources, and their ubiquitous availability has made them a viable alternative to existing commercial fossil fuels(Yadav & Reddy, 2020).

Hydrothermal carbonization (HTC) is the process of degrading organic matter by treating the reacting biomass components in water at a specific temperature and pressure to maintain the water in either a subcritical or supercritical state. HTC (also called wet torrefaction) is a technique for altering organic waste into a carbon-rich solid. Hydrothermal carbonization is accomplished at 180–260 ℃, with feedstock inundated in water and heated in a restricted enclosure for 5–240 minutes under 2–6 MPa (Libra *et al.,* 2011). HTC helps to prevail over the energy costs connected with drying the biomass since the process is aqueous based. HTC

is commonly recommended as a method for converting a variety of wet biomasses. Typically, HTC has been widely applied to convert biomass into energy. In co-hydrothermal carbonization (Co-HTC), two or more materials that have synergy are made to undergo HTC together. Typical feedstocks include Biomasses such as watermelon and pineapple peels (Azaare *et al.,* 2021), water hyacinth, and sewage sludge (C. Zhang *et al.,* 2020). 2); Biomass and plastics such as pomelo peels and PVC (Ning et al., 2022a); Sewage sludge and biomass such as sewage sludge and coconut shells (Tu *et al.,* 2021); Sewage sludge and Chlorella Vulgaris(Du *et al.,* 2021), and so on.

HTC simulates natural coal formation by transforming organic material in a primarily water-based feedstock into a coal-like substance one million times quicker than nature (Libra *et al.,* 2011). HTCs are affected by reaction parameters such as temperature, type of feedstock, resident time, and mixing ratios. *Gao et al*. (2013) looked at the impact of reaction time on the chemical and structural properties of hydrochar produced by hydrothermal carbonization of water hyacinth and found that after 4 hours, the chemical and physical properties of WH were unaffected by resident time. However, more significant parameters are the temperature(Yao & Ma, 2018, Zhao *et al*., 2020, Azaare *et al*., 2021) and the type of feedstock(Shen, 2020b). Mixing ratios have a significant impact on the yield of biochar where there exists a synergy between the feedstock used in a co-HTC. Increasing pressure had little to no effect on the HTC process.

Work has been conducted on the co-HTC of plastics and biomass feedstock. This is the first of its kind of valorisation study on the waste from Polyvinyl chloride and the plant Pontederia crassipes through co-HTC. In this work, high-energy hydrochar is produced from the co-HTC of Polyvinyl chloride and the plant *Pontederia crassipes*, varying the temperature (200- 260 ℃), resident time (60 – 120 min), and mixing ratio of feedstock (PVC: WH, 1:1-1:13). The thermal properties of the products were analysed to ascertain the optimal operating parameters by using the response surface methodology.

1.2 Problem Statement and Justification

The increase in population has increased energy demand and the corresponding rise in waste generation. Global waste generation is currently about 3.4 x 10^9 metric tonnes. This amount is expected to double in 2050 (World Bank, 2020). An effective way to slow down the accumulation of waste and reduce its effect on the environment is to convert the waste into a more useful form such as energy. Due to their versatility, lightweight and low cost of production relative to other materials such as metals, concrete, and wood, the dependency on plastics has increased over the years (Al-Salem *et al*., 2017). PVC, a popular plastic, is widely used in packaging, building, construction, automotive, and agriculture. It is frequently used in construction compared to the usage of polystyrene (PS) and polyethylene(PE) (*Plastics – the Facts 2020*, 2020), increasing PVC-containing wastes.

Many countries use landfills and incineration as a way of disposing of plastic waste to reduce expenses. Landfills are not sustainable due to their destruction of the soil structure, difficulty in decomposing, adverse effects on vegetation, and the exceeded occupation of land. Rainwater can penetrate landfill layers and contact the waste plastics containing different addictive, which will result in hydrophilic poisons dissolving in the leachate. As for burning, poisonous chemicals such as dioxins, furan, and heavy metals could be liberated into the atmosphere triggering a devasting effect on the environment, humans, and flora and fauna.

The hydrothermal carbonization (HTC) process can remove chlorine from PVC by dissolving it in the water thereby preventing the release of dioxins into the atmosphere (Poerschmann *et al*., 2015a). Although it is efficient to eliminate chlorine from PVC waste by HTC, alkalis are usually needed to enhance the dechlorination efficiency(Huang *et al*., 2019a). Lignocellulose biomass generally includes a high amount of alkali and alkaline earth metals (Shen, 2020b).

Water Hyacinth (*Eichhornia Crassipes*), an invasive aquatic plant, has a high percentage of lignocellulose and can therefore be a useful source of biomass for producing energy through HTC. WH is a fast-growing aquatic plant, which is projected to cover four (4) million hectares of water bodies (Bote *et al*., 2020). WH poses a challenge to humans by disrupting transportation and tourism, blocking irrigation systems, impeding drainage, and choking hydroelectric dams.

Co-hydrothermal carbonization of PVC and WH will not only ensure the safe disposal of PVC and removal of the nuisance plant but will also lead to the production of high-energy hydrocar, as an efficient waste energy product.

1.3 Objectives

1.3.1 Main Objective

The main objective of the study is to optimize the process parameters to produce high-energy hydrochar from waste polyvinyl chloride and Water hyacinth through a co-hydrothermal carbonization process.

1.3.2 Specific Objectives

The specific objectives of the study are to:

1. Optimize the process parameters to produce hydrochar by co-hydrothermal carbonization of PVC and Water hyacinth (WH) using the response surface methodology.
2. Determine the yield of hydrochar under different operating parameters.
3. Assess the High Heating Values (HHV) of the hydrochar under different operating parameters.
4. Quantify the dehalogenation efficiencies under different operating parameters.
5. Assess the effect of varying temperatures on the chemical composition of hydrochar by Fourier Transform Infrared microscopy.
6. Compare the thermal properties of the hydrochar.

1.4 The Scope and Limitation of the Study.

This study focuses on the valorisation of waste polyvinyl chloride and water hyacinth into high-energy hydrochar. An extensive study on the thermal properties of the hydrochar, which involves: The High Heating Values, combustion properties, and the removal of inorganic materials were studied using the thermographic analyzer, calorimeter, and FT-IR. The parameters that are varied during the co-hydrothermal carbonization are temperature, residence time, and mixing ratio. The other uses of the hydrochar such as for soil amendment, and producing supercapacitors, are out of the scope of this study.

1.5 Organization of the Study

The organization of this work is into five chapters. The first chapter gives an introductory background, the status quo of hydrothermal carbonization of plastics and biomass, and the scope and limitations of the work. Chapter two reviews relevant literature in the study. Chapter three looks at the materials and the methodology used in the study. This include the experimental study of co-hydrothermal carbonization of PVC and WH under varying operating parameters. Chapter four present results from theoretical and experimental studies. Chapter five present a synopsis of the findings, the conclusion of the study, recommendations made, and some consideration for future studies.

CHAPTER TWO

LITERATURE REVIEW

2.1. Hydrothermal carbonization

A thermochemical procedure called hydrothermal carbonization (HTC) is deployed to convert biomass with high moisture content so that it will be used in a variety of applications. The biomass is heated under pressure for 5-240 minutes while submerged in water at a temperature between 180 and 350 °C during HTC (Arellano *et al*., 2016). Other products are liberated during the process; however, the primary output of HTC is a substance called hydrochar. Additionally, it generates gas (mostly CO_2) and liquid (aqueous soluble) by-products (Fiori *et al*., 2014). The HTC can be operated with or without a catalyst, thus the procedure can be classed as either Direct HTC or Catalytic HTC. When HTC is performed in the absence of a catalyst, the feedstock is only mixed with water and heated in an enclosed reactor with varying degrees of temperature.

As depicted in Figure. 2.1, the subcritical zone is where the HTC process takes place. It is well established that the properties of water alter considerably under a subcritical state. Increases in temperature below 374 °C result in a reduction in the dielectric constant, which weakens the hydrogen bonds in water and creates high ionization constants that speed up the dissociation of water into acidic hydronium ions (H_3O^+) and basic hydroxide ions (OH^-) (Marcus, 1999).

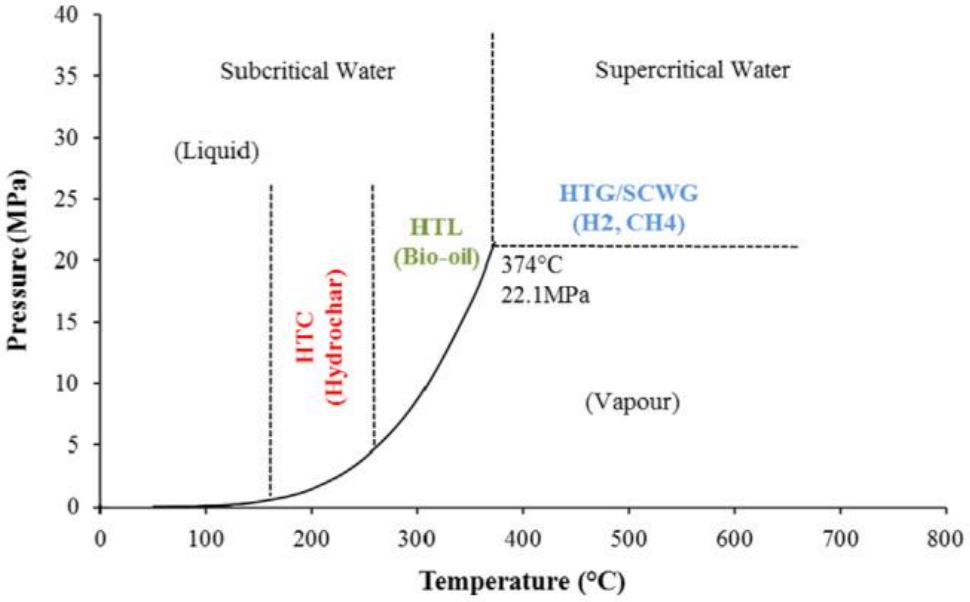

Figure 2.1 Schematic diagram for Hydrothermal Carbonization process.

Additionally, subcritical water is a good medium for the acid-catalysed reaction of organic compounds without the need for additional acid since it has an adequately higher H^+ concentration than liquid water (Ruiz *et al*., 2013). Water characteristics change substantially under different temperatures. Water provided to the process or found in the biomass acts as a good solvent and reaction media during HTC (Libra *et al*., 2011)

Several reactions take place during the reaction, and the exact kind of reaction pathways is yet undetermined. However, because hydrolysis has a lower activation energy than most other processes, it may be claimed that hydrolysis governs the HTC (Heidari *et al*., 2019). Many bonds are broken during the reaction. In the hydrolysis process, the ester and ether bonds of the hemicellulose (at Temperature > 180 ℃), cellulose (at Temperature > 200 ℃), and lignin (at Temperature > 220 ℃) break into several fragments (Titirici & Antonietti, 2010). Dehydration and decarboxylation proceed with the pyrolysis reaction, and they are responsible for reducing H/C and O/C ratios (Matus *et al*., 2016). Water can enter the reaction medium due to dehydration. The dehydration of glucose is depicted in Equation 1. (Titirici, 2006)

$$C_6H_{12}O_6 \longrightarrow C_6H_4O_2 + 4H_2O \qquad (1)$$

Decarboxylation reaction leads to the degradation of carboxyl and carbonyl groups and the evolution of CO_2 and CO. Condensation polymerization immediately follows decarboxylation, which involves the participation of some of the fragments of the previous reactions. The combination of molecules occurs, resulting in the simultaneous formation of a larger molecule and the release of a small molecule. Furthermore, aromatization processes produce aromatic polymer structures that are hydrothermally stable and are used to construct hydrochar (Tekin *et al*., 2014). It is worth mentioning that the central difficulty in knowing the interaction of hydrothermal carbonization is that the reaction processes do not happen in sequence and their order, difficulty, and relations are not revealed yet (Sevilla & Fuertes, 2009).

2.2. HTC Processes

Even though the reaction pathway for hydrothermal carbonization is not fully studied, many scientists agree that the main reactions that occur in the process are hydrolysis, dehydration and decarboxylation, condensation and polymerization, and aromatization (Pauline & Joseph, 2020). HTC's products are mostly made up of three states: solid, aqueous solution (bio-oil combined with water), and a little amount of gas (mainly CO_2). The major product of HTC is solid residue, which may be easily isolated from the solution due to its strong hydrophobicity and homogenous characteristics (Hoekman *et al*.,2013).

2.3. Co-hydrothermal carbonization

Co-HTC is the thermochemical alteration of two or more feedstocks in a suspension with water under saturated pressure for many hours at a moderate temperature (200-300 ℃) (Tekin *et al*., 2014). The primary distinction between HTC and co-HTC mechanisms is that in co-HTC, many feedstocks are employed, whereas, in HTC, only one material is considered. Azaare *et al*. (2021), did co-hydrothermal carbonization of pineapple and watermelon peels. Xu *et al*. (2021) produced solid fuel from the co-HTC of textile waste and polyvinyl chloride waste. Even though most of the feedstock used was mainly from solid sources, some of which have to undergo side reduction, other works have been done on liquid feedstocks. Du *et al*. (2021) worked on the effects baking soda has on the co-HTC of sewage sludge and *Chlorella vulgaris*. Other studies include sewage sludge and polyvinyl chloride (Zhang *et al*., 2020), sewage sludge and fuel addictive (Wilk *et al*., (2021), and

sewage sludge and coconut shells (Tu *et al*., (2021). Results from all these co-hydrothermal carbonizations of feedstocks have several advantages over when only a single feedstock is hydrothermally carbonized.

Hydrothermal carbonization reactions are favoured in the acidic medium through its main reaction path of dehydration and decarboxylation reaction. Biomass used as feedstocks in the co-hydrothermal carbonization process creates a favourable acidic medium to catalyse the reaction process (Lynam *et al.*, 2015). Hydrochars produced from the co-hydrothermal carbonizations of two or more feedstocks have better fuel properties than when a single feedstock is hydrothermally carbonized. Co-HTC provides a safer medium for disposing of chlorinated waste without polluting the environment. According to Poerschmann *et al*. (2015b), Polychlorinated dibenzodioxins (PCDDs) and dibenzofurans (PCDFs) were not detected from the hydrochar produced from the hydrothermal carbonization of polyvinyl chloride.

2.4. Raw Materials for Co-HTC

Biomasses are living or recently living organic materials mostly made of carbon, hydrogen, and oxygen that have molecular bonds that store solar energy. The highest usage potential of all renewable energy sources is found in biomass. Agricultural and industrial activities generate a high percentage of waste biomass. Other examples of biomass are algae, grass, rice, cassava, plantain, urban waste, and agro-industrial wastes. Biomass can also generally be referred to as all living or recently deceased organisms and their wastes. Biomass is a cleaner source of energy and has a high usage potential as a substitute for fossil fuels and will be the most common energy source in the future (Tekin & Karagöz, 2013).

According to Bardhan *et al*. 2021, the lignocellulosic biomass having complex carbohydrate structures as well as agro waste (peels, crowns, sticks, etc.), including woody deposits, are typically chosen for co-HTC. Because of their incessant supply, low cost, and renewability, these materials have received a lot of attention. Yang *et al*.(2019) classified the biomass that has been used in the study of hydrothermal liquefaction into seven categories. Agricultural waste and residues, forest residues, food processing wastes, livestock waste, algae, sewage,

municipal solid waste, and plastic trash are the categories. Wastes from agricultural sources are abundant and can easily be obtained from agricultural activities.

Most agricultural waste comprises a high concentration of cellulose and hemicellulose compared to the lignin content (10-20%), but the lignin concentration of wood trash contains a high concentration of lignin (30%) (Yang *et al*., 2019). Furthermore, the lower percentages of sulphur and nitrogen in most agricultural waste compared to the carbon (C) content allows these types of material materials to be converted into more latent hydrochar with higher heating values and meaningfully lower poisonous gases (Liu *et al*., 2013). Biomass with high volatile matter (VM) yields result in reduced efficiency and higher emissions of contaminants (Khan *et al*., 2019). Except for some commercial coal varieties, the fixed carbon (FC) of agro- and wood-residues is significantly higher than that of other biomasses. Because of its synergistic blending effect, the co-HTC method may control such benefits and downsides of separate materials collectively (Sevilla & Fuertes, 2009).

To date, sewage sludge is the second most often used material in the co-hydrothermal process. The mineral content of sewage sludge varies depending on the site of supply, ranging from 21 to 52 percent and 17-56 percent, respectively (Bardhan *et al*., 2021). Dewatering is more difficult because of the high ash concentration and low organic matter, and this problem incumbents the entire resource recovery method (L. Wang *et al*., 2019). Aside from that, it is insufficient for possible energy sources because of the small surface area, low heating value, and high heavy metal concentration of sewage sludge char (Li *et al*., 2016). Scientists have proposed the co-HTC technique for improving sludge quality to overcome the challenges outlined here, in which sewage sludge is combined with other biowastes or high-graded coal (Song *et al*., 2019b).

Due to their low production cost, good feasibility, low density, and robustness, plastics, a synthetic polymer, are abundant substances in modern life. However, low biodegradability and adaptability cause management challenges, as well as significant environmental impact. PVC is currently widely disposed of in landfills and by incineration. Toxic emissions are produced by combustion/pyrolysis processes used to dispose of PVC, as well as the production of inorganic chlorine, which causes corrosion in the furnace (Poerschmann *et al*., 2015a). As a result, a dependable alternative approach for securely and efficiently treating

PVC waste in an ecologically sound manner is worthwhile to pursue. Hydrothermal carbonization provides a useful solution to these problems.

PVC, like all other plastic pollutants, is steady and includes a high concentration of chlorine (Cl) (35-48 percent), putting a strain on the ecology (Lu *et al.*, 2020). Scholars have proposed a co-HTC method utilizing PVC rather than only HTC for clean solid fuel generation in this regard. Blending has a favourable synergistic impact on removing organic Cl content and another inorganic with high yield output (Huang *et al.*, 2019b).

2.5 Hydrochar and Biochar

The history of biochar may be linked to the ancient people of the Amerindian of the Amazon area, referred to locally as Terra Preta de Indio when black soil was generated using slash-and-burn practices (Ahmad *et al.*, 2014). Biochar is a brand-new scientific word. According to Lehman and Johnson (2009), when biomass such as sawdust, dung, or leaves is subjected to a high temperature in a closed container with limited or in the absence of air, biorochar is produced. The International Biochar Initiative (IBI) guidelines currently govern the most standardized definition of biochar, which states that "biochar is a solid material obtained from the thermochemical conversion of biomass in an oxygen-limited environment."(IBI, 2015).

Hydrochar, on the other hand, is a product that is like biochar but is formed using a completely different pre-handling process and circumstances. Biochar is normally created as a solid by-product material after a dry carbonization process such as pyrolysis, whereas hydrochar is formed as a slurry (a combination of solid and liquid) during an HTC process (Kambo & Dutta, 2015).

2.6 Uses of hydrochar

2.6.1 Power generation

The Hydrothermal Carbonization process can transform the raw materials (mostly biomass feedstock) into a new product that is coallike having better thermal and physicochemical properties. As a result, this new product can be used in place of coal for energy production (Reza *et al.*, 2014). The high heating values of the resulting product of the hydrothermal

carbonization process are increased when hemicellulose and cellulose are removed from the biomass. This results in an increase in the C/O ratios as the temperature increases. Kambo & Dutta, (2014) observed a complete hemicellulose degradation during the HTC process, ensuing in a product with higher lignin content, which serves as a natural agglutinate and aids in energy compaction. HTC can eliminate some of the non-combustible alkali materials that are major contributors to the development of ash during combustion. Creamer & Gao, (2016) found that adding hydrochar to raw biomass improves combustion characteristics by removing a significant quantity of volatile matter and growing carbon content. Their findings further showed that adding hydrochar and coal would result in a reduction in gaseous emissions contaminants, specifically carbon dioxide, methane, sulphur dioxide, nitrogen oxide, and carbon monoxide.

Furthermore, the thermogravimetric analysis of hydrochar revealed that an increase in the process temperature increased the ignition combustion of the hydrochar because of the greater reduction in the volatile matter. A comparable trend was observed for burnout temperature as fixed carbon increased. Yang *et al*. (2019) conducted similar research and produce more detailed results on the combustion kinetics of hydrochars.

2.6.2 Separation of gases and Carbon sequestration

According to Creamer & Gao, 2016), hydrochar can be used to separate gases from flue gas streams including carbon dioxide, hydrogen sulphide, and nitrogen, or to eliminate heavy metals and pollutants from water, particularly if it is substantially stimulated or stimulated through acidic/alkaline instigation process The HTC method may be tweaked to create hydrochar with appropriate characteristics contingent on the kind of pollutants intended for removal. Demir-Cakan *et al*. (2009) discovered that When glucose is hydrothermally carbonized using acrylic acid as a catalyst can produce hydrochars that can be used to eliminate heavy metals such as Cd^{2+} and Pb^{2+} from contaminated water. Therefore, to use hydrochar as an adsorbent material, its physical properties such as surface area, surface charge, and surface functionality are the primary considerations for using hydrochar as an adsorbent.

The process of converting a biomass feedstock to biochar and then storing it in a reservoir such as soil is known as carbon sequestration or carbon capture and storage (Glaser *et al*.,

2001). According to Glaser *et al.* (2001), the soil is a major carbon sink that serves as a reservoir of carbon captured. Oceans significantly serve as carbon storage which helps to capture carbon dioxide in the atmosphere thereby helping to mitigate the effect of global warming and climate change (Hu *et al.*, 2022). The carbon captured and stored in the soil, oceans, and plants embodies a net elimination of carbon from the atmosphere. Hydrochar is a good storage of carbon. The stability of the storage of carbon in hydrochar is increased at increasing temperatures. At higher temperatures, there is an increase in aromatization and dehydration which increases carbonization making it difficult for its decomposition (Cavali *et al.*,2023). The Terra-Petra soils of the Amazon region inspired the concept of biochar (carbon) sequestration. These soils are reported to have a significant amount of carbon (in the form of char) stored in the soil and improved microbial diversity when compared to nearby soils (Glaser *et al.*, 2001).

2.7 Factors affecting HTC

2.7.1. Effect of Temperature on HCT

The temperature of the co-HTC is a significant factor in the synthesis of hydrochar and in managing all reaction processes. High temperature provides enough heat to break down macromolecules into pieces that dynamically produce different chemical linkages. The temperature, however, has an opposing effect on the yield of hydrochar as the increase in temperature resulted in a decrease in the quantity of hydrochar produced. Research in the co-hydrothermal carbonization of pineapple and watermelon peels by Azaare *et al*. (2021) disclosed that the yield of hydrochar reduced rapidly from 57% to 44% when the reaction temperature intensified from 180 ℃ to 250 ℃. This declining tendency is also supported by Zhang *et al*. (2019) in the case of polyvinyl chloride and lignocellulose biomass.

Temperatures reaching a specific reaction level have a significant impact on the hydrolysis reaction of biomass, and high temperatures can result in simultaneous dehydration, decarboxylation, and condensation (Wang *et al*., 2018). According to Kang *et al*. (2012), the decarboxylation mechanism and partial breakdown of fallen leaves in the liquid phase might be associated with this reduction. It is worth mentioning that the yield obtained from the sludge-microalgae combination decreased substantially from 93.88% to 46.76% with the temperature increasing from 180 ℃ to 270 ℃ (Lee *et al*., 2019).

During the reaction, when the temperature required to disintegrate the primary constituent of the feedstock is insufficient, a pyrolysis-like process, as opposed to the reaction of the monomers during the homogenous reaction, is likely to occur. Temperatures of 200 °C, for example, resulted in minimal cellulose breakdown, resulting in a partial pyrolysis-like reaction (Bobleter, 1994). The solid output declines steadily as the temperature rises, but the liquid and gaseous products increase. At temperatures higher than the HTC temperature, the process is known as hydrothermal liquefaction, and the yield of the liquid product is greater than the solid and gas yields, with the yield of gas dominating as the temperature rises as a result of the intensification of thorough processes (Heidari *et al.*, 2019).

2.7.2 Residence Time

Residence time is the period during which the reaction commences to when the reaction is interrupted under a given operating parameters. It is one of the most significant factors that affect hydrothermal carbonization reactions. It has been found in research that when the residence time is prolonged, a low amount of product is formed (Gu *et al.*, (2018), Wang *et al*. (2020b)). Thus, residence time has an inverse relation with the yield of product in hydrothermal carbonization reactions. An increase in residence time resulted in an increase in carbon content from 52.24% to 62.77% within the period of 1h to 10h, whiles oxygen content decreased from 40. 29% to 28. 13 at the same reaction conditions (Liang *et al*., 2020). This results in the decline of the H/C and O/C ratios of the resulting products (Shen, 2020a). Gao *et al*. (2013) showed that residence time enhanced the structural properties but had little effect on the chemical properties of the hydrochar that is produced.

2.8 HTC reactors

The reactors that are used for Co-HTC reactors have different variations based on their size and design. Figure 2.2 shows the schematic diagram of an HTC reactor. Some of the most common types of reactors are hydrothermal autoclave reactors, stainless steel autoclave reactors, polytetrafluoroethylene-lined stainless autoclave reactors, and Teflon-lined autoclave reactors (Bardhan *et al.*, 2021). In a laboratory-scale setting, the capacity of the reactor cubicle can range from 30 mL to 1 L. The reactor chamber is loaded with a predetermined ratio of feedstock and water. The reacting vessel is then placed in a layer that

has an insulating layer in a closed system. The compartment lid usually has stirrers which control the shaking speed when the reactor is operating. Modern reactors have a control panel that is used to control the reaction conditions inside the reacting vessel.

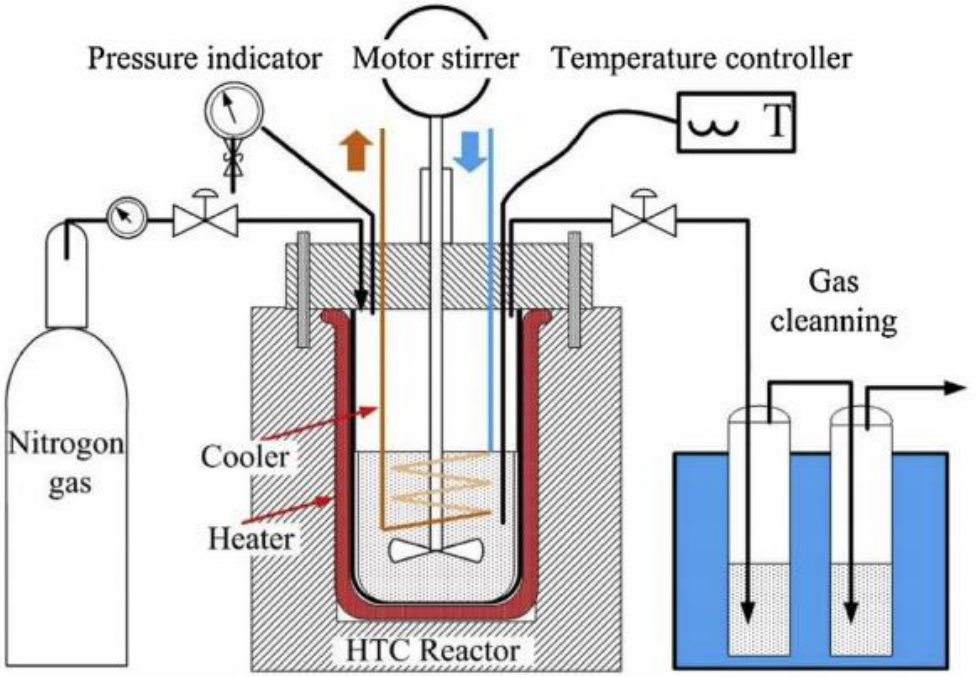

Figure 2.2. System schematic of a hydrothermal carbonization autoclave reactor

Source: (Ma et al., 2019)

2.9 Plastics Production

Plastics are artificial organic polymers that are mostly produced using petrochemical feedstock. Leo Hendrik Baekeland created the first plastic, Bakelite, in 1909; it is now called phenolic resin (Roadmap, n.d). Bakelite's use expanded quickly. Products like telephones and pot handles have been made with them. A growing plastics industry was built on the chemistry of combining tiny molecules into macromolecules.

The German I.G. Farben Company created synthetic rubber known as Buna-S, polyvinyl chloride, and polystyrene between 1920 and 1932. Du Pont made a breakthrough in 1934 when it unveiled nylon, a substance that was finer, stronger, and more elastic than silk. By 1936, businesses in Germany, Britain, and the United States were manufacturing acrylics. Polyethylene was created in the same year by the British business Imperial Chemical

Industries. Friedrich Bayer & Co. of Germany developed polyurethane in 1937, but it was not made commercially available to consumers until the 1950s thanks to American businesses. Polyepoxide (also known as epoxy) was first patented in 1939 by the German company I.G. Farbenindustrie, but it was not made commercially available until almost four years later by a U.S. corporation.

The frequency of new polymer discoveries increased following World War II (1939–1945). Polyethylene terephthalate was created in 1941 by a modest English business. The use of Polyethylene terephthalate did not become common until the 1970s, even though Du Pont and Imperial Chemical Industries manufactured Polyethylene terephthalate fibres (marketed under the names Dacron and Terylene, respectively) after the period of the war. Bayer and General Electric's post-World War II research led to the creation of polymers like polycarbonates, which are used to create small appliances and safety helmets. Polysulfide, a linear, heat-resistant thermoplastic first made popular by Union Carbide Corporation in 1965, is used to create hospital equipment that can be autoclave sterilized as well as face shields for astronauts (a device that uses high-pressure steam for sterilization).

Plastic characteristics can now be tailored to a variety of design parameters by scientists. Artificial joints, contact lenses, space suits, and other specialty materials are made with modern polymers. Plastic use has increased as they have gotten more versatile.

In 2019, global plastics production reached 370 million tonnes, with the Middle East and Africa contributing only 7% of the production. The industry reached a positive trade balance of more than thirteen billion euros in 2019 (UNEP,2018).

2.10. Types of Plastics

2.10.1 Thermoplastics

Thermoplastics are groups of plastics that melt upon heating and solidify when the source of heat is removed. The properties that give the substance its term is reversible. That means, it can be repeatedly warmed, moulded, and solidified. Thermoplastics have low molar mass giving them a low melting temperature and a low melting velocity (Eyerer, 2015).

2.10.2 Thermosets

Thermoset plastics experience a chemical transformation when heated, producing a three-dimensional network. After they are heated and shaped these plastics cannot be re-liquefied and renewed. Table 2.1 shows examples of these two types of plastics.

Table 2.1 Types of plastics

Source: Kameel *et al*., (2022)

Thermoplastics	Thermosets
Polyethylene (PE)	Polyurethane (PUR)
Polypropylene (PP)	Epoxy resins
Polyethylene Terephthalate (PET)	Vinyl esters
Polystyrene (PS)	Unsaturated polyesters
Expanded polystyrene (EPS)	Melamine resins
ABS	Silicone
SAN	Phenol-formaldehyde resins
Polyamides	Urea-formaldehyde resins
Polycarbonate	Acrylic resins
Polymethyl methacrylate (PMMA)	Phenolic resins Etc.
Thermoplastic elastomers (TPE)	
PEEK, POM, PBT, EVOH Etc.	

2.11 Water Hyacinth

Water hyacinth (*Pontederia crassipes*) is a floater with bright green, waxy leaves and lovely violet blooms with yellow stripes on the notable petals (Heidari *et al*., 2019). These plants form a layer on the surface of the water that they cover. Water hyacinths can sometimes grow in areas close to the edge of a water body or pocket of stagnant water. The arrangement of the leaves is in a form of a rosette. The stem has spongy tissue which creates a mostly hollow section that makes them buoyant. The leaf stem of mud-anchored plants is not swollen.

Currently, getting an appropriate biomass feedstock for biofuel creation by depicting the unique biofuel properties of the feedstock is a significant challenge. Nonedible feedstocks such as lignocellulosic biomass or aquatic biomass have gained popularity in recent years as a way to avoid the environmental and food security risks accompanying carbohydrate-rich food crops (Sahoo *et al*., 2019). Recently, researchers all over the world have attempted to use aquatic feedstock to produce bio-fuel/chemicals(Kaur *et al*., 2018). Vanavanichkul *et al*. (2021) did a stepwise conversion of water hyacinth waste to carbon Nano horns by a combination of hydrothermal action, carbonization, and arc in water processes, and converted the dried water hyacinth with a carbon content of 39% to hydrochar with a carbon content of 57%. Román *et al*. (2020) studied the Appropriateness of hydrothermal carbonization to change water hyacinth into added-value products. The study reveals that hydrothermal carbonization can deliver a sustainable green path to yield added-value materials from Water Hyacinth.

Several processes have been investigated in the energy field to change WH into biofuels. WH has mostly been studied as a biogas generation substrate; in this regard, some encouraging outcomes have been recorded when the weed is combined with other biomass such as cow dung and elephant grass (Okewale *et al*., 2016). Bioethanol synthesis from both virgin and processed WH has also been shown (Das *et al*., 2016). Lately, the synthesis of biohydrogen from WH has also been studied, with encouraging findings (Pattra & Sittijunda, 2015). Briquette manufacturing from WH for household combustion processes (Ighodalo *et al*., 2011) has also been reported. In the latter situation, WH must be blended with other materials to produce appropriate combustion characteristics.

CHAPTER THREE

MATERIALS AND METHODS

3.1 Materials, Chemicals, and Equipment

3.1.1 Raw Materials

The raw materials used in this study are Polyvinyl chloride (PVC) and Water Hyacinth. The PVC was obtained from PVC pipes from the KNUST plastic recycling plant. The water hyacinth was obtained from the Jeoun lagoon in Jaway Wharf, which is in the Jomoro District of the Western region of Ghana in January 2021.

3.1.2. Chemicals

Various reagents were used during the laboratory analysis of the biomass. Some of the chemicals used for the study are sodium carbonate and sodium bicarbonate.

3.1.3 Equipment used.

For the hydrothermal carbonization, a 100 ml stainless steel (Figure 3.2 b) autoclave reactor was used. It consisted of the Teflon reacting chamber, the autoclave body, treaded cap, the upper and lower disk, and a rob for locking. The autoclave with its content is placed in a Muffle furnace (Nobertherm Electronics, Germany) (**Error! Reference source not found.**).

3.2 Raw Material Preparation and Characterization

3.2.1 Powdered Water Hyacinth

The fresh Water hyacinth was washed with water and dried at 105 ℃ for 24 hours using an oven dryer as shown in Figure 3.1 a. It was then milled using a hammer mill (Figure 3.1 b) and seized to 500 *u*m particle size. The powered WH was sealed in a transparent plastic bag.

Figure 3.1. (a) Oven dryer used to dry the WH, (b) A hammer mill used to mill the WH.

3.2.2 Sample Preparation-Powdered PVC

The pipes were dried for 72 hours and crushed to obtain particle sizes of 500 um. The powered PVC was stored in a transparent plastic bag for later use.

3.3 Proximate analysis of Water Hyacinth and PVC

3.3.1 Moisture Content-Water Hyacinth

The ASTM standard was employed in the estimation of the moisture content of the raw material. 50 g of water hyacinth was positioned in the oven at 105 ℃ for 24 hours. The process was replicated three times. The following expression was then used to calculate the moisture content of the samples:

$$MC = \frac{m_i - m_f}{m_i} x100 \qquad (2)$$

Where

m_i is the initial mass of the biomass (in grams (g))

m_f is the final mass of the biomass after drying (in grams (g))

3.3.2 Ash content

The ash content was determined following the ASTM Standard.5g of sample was heated to 550 ℃ for 4 hours and cooled below 200 ℃ and maintained for 20 minutes. The ash content was calculated as follows:

$$(A + B) - A = B \quad (3)$$

$$(A + C) - A = C \quad (4)$$

$$\% \, Ash = \frac{C}{B} x \, 100 \quad (5)$$

where A = crucible weight (g),

B = sample weight (g),

C = ash weight (g).

3.3.3 Volatile content

The volatile matter was determined following ASTM D5832-98 (2014). About 2 g of each of the biomass constituents with particle size 425 µm, was placed in a porcelain crucible. Each sample was initially oven dried and then retained in an electric furnace at a temperature of 550 ℃ for 10 minutes and weighed after cooling in a desiccator. The percentage of the volatile matter was then calculated using the equation below.

$$\text{Volatile matter } (\%) = \frac{E - \text{F}}{E} \times 100 \quad (5)$$

Where: *E* =Mass of Sample after drying at 105 ℃ (g)

F = Mass of Sample after drying at 550℃ (g)

3.4.0 Experimental Design

The experiment was designed to determine how modifying the temperature, reaction time and biomass ratio will affect the chemical and thermal properties of the hydrochar produced by co-HTC. The temperature ranged from 200–260 ℃, the time, from 60–120 min, and using the biomass ratio from 1:3–3:1, respectively. When the boundaries of the parameters were selected, the Box Behnken Design method was used to generate the experimental points. The Design of Experiment software (version 13) was used to determine the number of runs. A total of 17 runs were obtained.

Figure 3.2. (a) Parts of the autoclave reactor, (b) Stainless steel autoclave reactor used for the Co-HTC.

For a comprehensive evaluation of the co-HTC process, the following output variables were chosen to respond to the changes in the Co-HTC reaction conditions: The yield of hydrochar, dichlorination efficiency, higher heating value (HHV) (or calorific value), and energy densification ratio (EDR).

3.5 Co-carbonization process

For each treatment, 5 g of the feedstock was loaded into the reactor and 70 ml of distilled water was added. The autoclave reactor used has an inner Teflon volume of 100 ml. The PVC and water hyacinth were in the ratio of 1:3, 1:2, and 1:1. The mixture in the inner Teflon container was stirred for 5 minutes to obtain a slurry mixture. When the furnace was heated to the pre-set temperatures of 200 ℃, 220 ℃, and 260 ℃, the reactor was placed in it to allow for the carbonization process for the pre-set time of 60, 90, and 120 minutes. Once the reaction time has elapsed, the autoclave is removed from the furnace and cooled to room temperature using water. The autoclave was opened to allow the gasses to escape, and the mixture was filtered using 0.7*u*m filter paper. The filtrate was dried at 105 ℃ for 24 hours before being grounded and separated to a size diameter range of 0-500 *u*m for further analysis. Each experiment was replicated three times for accuracy.

Figure 3.3. (a) The raw PVC and WH feedstock, (b) Samples of Hydrochar produced by Co-HTC of WH and PVC

3.5.1 Hydrochar Yield

The hydrochar yield from the Co-hydrothermal carbonization was calculated using Equation 2

$$\text{Hydrochar yield} = \frac{\text{Mass of hydrochar (g)}}{\text{Mass of feedstock (g)}} x\ 100 \qquad (6)$$

3.5.2 Energy Content and Energy Densification Calculation

The modified Dulong formula was used to calculate the energy content (calorific value) of the feedstocks and hydrochar (Hosokai *et al*., 2016).

$$CV = 0.382C + 0.849\left(H - \frac{O}{8}\right) \qquad (7)$$

where CV = Calorific value of bio-chars (MJ/kg),

C, H, and O = mass percentages of Carbon, Hydrogen, and Oxygen, respectively.

3.6 Dechlorination Efficiency

The chlorine concentration in the hydrochar was measured using ion chromatography following EN 14582:2007 (Lu *et al*., 2021). When the samples were ignited with ethanol,

the organic chlorine was changed. It is then dissolved in a solution of sodium carbonate and sodium bicarbonate. The dissolved chlorine was then measured using ion chromatography. The following equation was used to calculate the dechlorination efficiency:

$$\mathrm{DE} = \left(1 - \frac{Mass\ of\ Chlorine\ in\ Hydrochar}{Mass\ of\ Chlorine\ in\ Feedstock}\right) x\ 100 \qquad (9)$$

3.7 Analysis of Functional Group

Using a Fourier transform infrared (FT-IR) spectrometer, the functional groups of raw biomasses and hydrochar were determined. The FT-IR spectrum was scanned using 24 scans at a spectral resolution of 4 cm^{-1} between 4000 cm^{-1} and 500 cm^{-1}.

3.8 Thermogravimetric Analysis

Beijing Hengjiu's HCT-4 microcomputer differential thermal balance was used to determine the combustibility of the various samples (Ning *et al*., 2022b). The sample was dried for 24 hours at 378 K before being ground to less than 74 mm. In the experiment, 5 mg of the sample was precisely weighed, added to the sample crucible, and then placed on a differential thermobalance with a heating rate of 20 ℃/min.

CHAPTER FOUR

RESULTS AND DISCUSSION

4.1 Optimization of Output Variables

The Design Expert software (Version 13) was for the optimization process, modelling the output variable, and undertaking the analysis of variance, using the response surface method. The Box Behnken Method was used to generate the experimental runs used for the iteration of the responses. The optimal conditions predicted from the data using the RSM are temperature, 230 ℃, residence time, 86 minutes, and mixing ratio of 0.33. These parameters were used for the confirmation and validation and the HHV obtained was 27.32 MJ/Kg

4.2 Effects of Process Parameters on Output Variables

4.2.1 Effect of Process Parameters on Dechlorination.

Table 4.1 shows the various varied combinations of the process parameters and their corresponding hydrochar that were obtained. The experimental errors of the data obtained are depicted by the normal plot of residuals and the residuals against predicted responses as shown in appendix 1 and 2.

Table 4.1 Combinations of process parameters

Std	Run	Temperature (^{0} C)	Residence Time (min)	Mixing ratio (WH/PVC)	Hydrochar Yield (%)	Dechlorination (%)	High Heating Value (MJ/Kg)
6	1	200	60	2:1	70.33	20.32	16.1642
11	2	260	60	2:1	31.34	93.66	30.0471
1	3	200	120	2:1	55.76	40.32	20.9986
4	4	260	120	2:1	30.01	95.67	32.3368
7	5	200	90	1:1	67.32	28.78	20.5837
2	6	260	90	1:1	30.12	94.39	30.948
3	7	200	90	3:1	65.48	25.54	18.2607

5	8	260	90	3:1	30.12	90.54	29.8569
13	9	230	60	1:1	40.34	80.33	26.696
15	10	230	120	1:1	33.57	87.22	29.2599
17	11	230	60	3:1	38.44	72.76	25.1316
8	12	230	120	3:1	32.69	85.87	27.508
10	13	260	60	2:1	31.25	93.54	29.6217
16	14	200	90	1:1	64.21	30.46	19.4176
14	15	230	90	2:1	35.66	84.69	26.3837
12	16	230	90	2:1	36.11	83.77	27.9965
9	17	230	90	2:1	36.32	85.69	27.1123

The normal plot of residuals of the variables is distributed in a straight line. The plots of residuals against predicted responses were intermittently distributed over and beneath the x-axis, signifying that the fitting of experimental results by the proposed models is within the acceptable level (Kang *et al*., 2019). Figure 4.2 shows the effect of temperature, residence time, and mixing ratio on dechlorination. The model that describes the effect of the parameters on DE is given as:

$$
\begin{aligned}
&Dechlorination\ efficiency \\
&= -1569.49427 + 12.72064\ Temperature \\
&+ 1.29576\ Residence\ time\ + 3.44809 Mixing\ ratio \\
&- 0.005253\ Temperature\ *\ Residence\ time \\
&+ 0.009565\quad Temperature\ *\ Mixing\ ratio \\
&+ 0.051833\quad Residence\ time\ *\ Mixing\ ratio \\
&- 0.024326\ Temperature\text{^}2 - 0.000112\ Residence\ time\text{^}2 \\
&- 3.07100\ Mixing\ ratio\text{^}2
\end{aligned}
$$

The results of the analysis of variance (ANOVA) of the output variables are displaced in Table 4.1. The temperature was the utmost leading factor having a p-value of < 0.0001 compared to residence time and mixing ratio. The response surface graph was visualized in Figure 4.2. The temperature had a positive influence on removing chlorine from PVC. The lowest DE 20.32% was recorded at 200 ℃, 60 min, and a ratio of 2. As the temperature was increased to 230 ℃, the DE was increased more than four times to 85.45%. The highest DE, 95.69% was recorded at 260 ℃. There was however a slight increase in the DE as temperatures were increased from 230 to 260 ℃. Dechlorination took place in two stages: elimination and substitution. Chlorine and hydrogen are removed from the two carbons in the vinyl structure by dehydrochlorination through the zipper mechanism to generate HCl. The hydroxyl (-OH) groups replaced the chlorine atoms on the polymer chain to produce C-OH groups (R2), which then reacted with oxygen atoms to form carboxylic acid (R3). If two hydroxyl (-OH) groups are substituted, HCl can be produced by intramolecular and intermolecular dehydration between these unstable intermediates (Zhao *et al*., 2017).

As a result, both elimination and substitution could produce acid substances, creating an acidic environment for inorganics removal. Cellulosic materials were decomposed during HTC and hydrolysed to produce 5-hydroxymethyl furfural or alcohol with a large free OH bond. According to Yao & Ma (2018), substances containing free OH improves improve the substitution route of the PVC reaction.

Residence time also had a significant influence on degrading PVC during the co-hydrothermal carbonization process. The dichlorination efficiency almost doubled from 20.32% at 200 ℃ to 40.32% when the time was doubled from 60 to 120 minutes.

When the time was increased to 90 minutes at the same temperature, DE increased to 30.46%. However, at higher temperatures, the effects of residence time on DE were minimal. At 260 ℃, the DE increased to 93.66%, 94.39%, and 95.67% when the time was increased to 60, 90, and 120 minutes, respectively. This means increasing both temperature and resident time can improve the dechlorination process in the co-HTC.

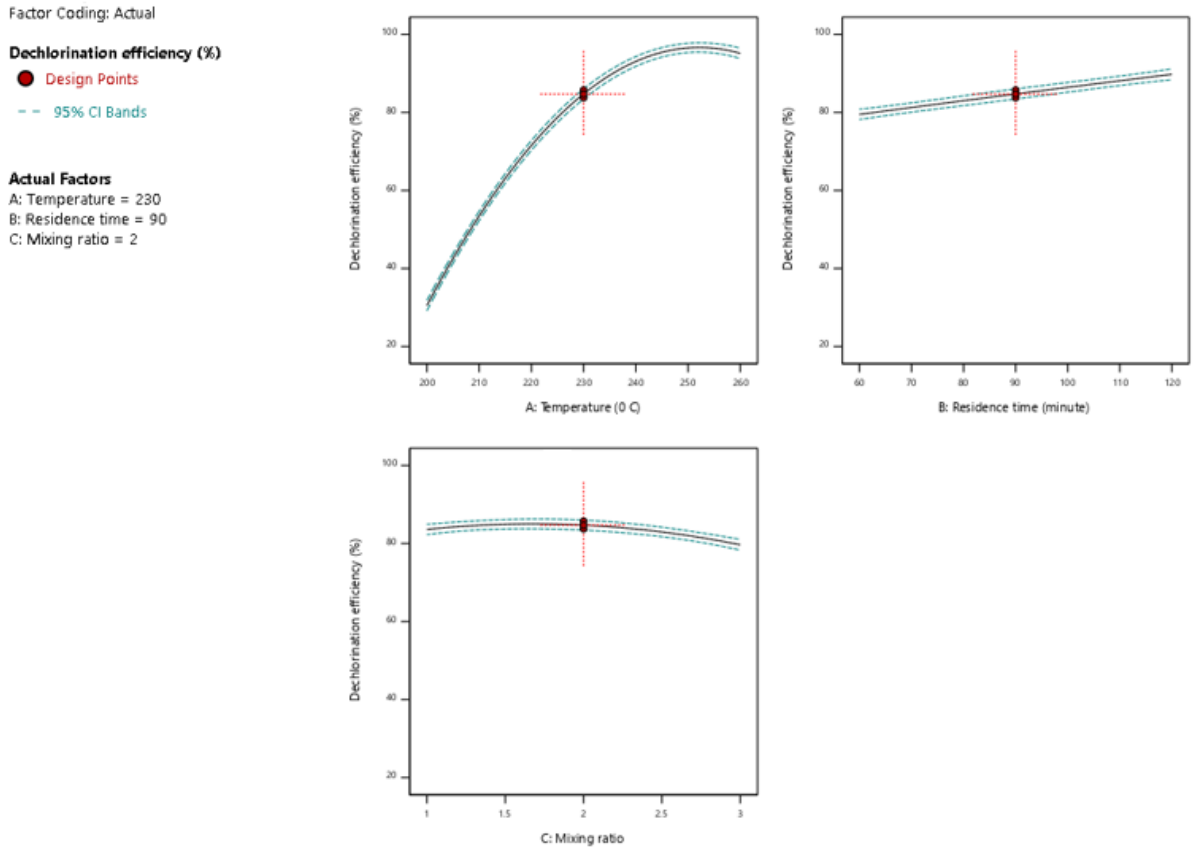

Figure 4.1 Effect of parameters on dichlorination efficiency in 2D

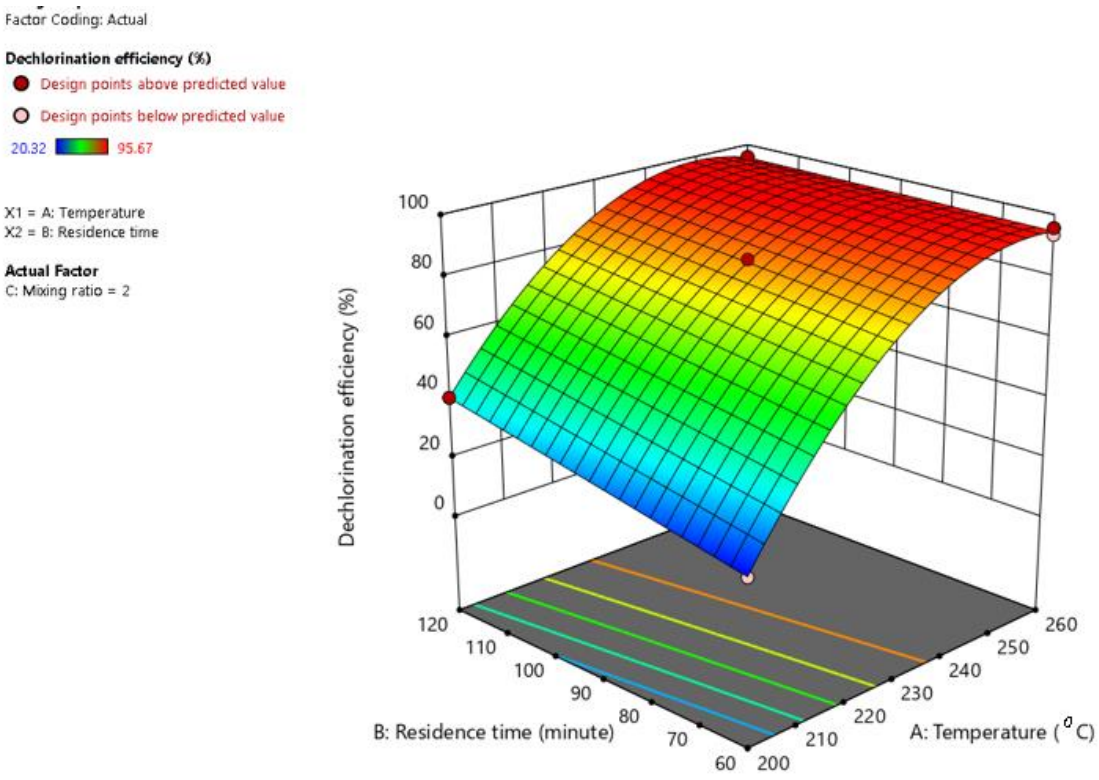

Figure 4.2 Response surface showing the effect of process parameters on dichlorination efficiency.

4.2.2 Effect of Process Parameters on Yield of Hydrochar.

PVC and water hyacinth in suspension with water were converted to hydrochar by co-HTC. Table 4.2 shows the output of the hydrochar yield at different operating parameters. Before analysing the exact outcomes, the normal residual plots (Fig. 4.9) and residuals against predicted responses (Fig. 4.10) were used to assess the experimental errors. They have a linear relationship with minor variation. These evaluations show that the model has a good fit for the experimental data. As a result, the developed models can be considered adequate for predicting and optimizing the biochar fuel production process, signifying that the residuals are normally distributed and thus confirming their normality(Anupam *et al.*, 2016). The model expressed in terms of actual factors for the yield of hydrochar is given as:

$$Hydrochar\ yield$$
$$= +919.58984 - 6.68607\ Temperature - 0.872349\ Residence\ time$$
$$- 4.65110\ Mixing\ ratio + 0.003494\ Temperature * Residence\ time$$
$$+ 0.005012\ Temperature * Mixing\ ratio + 0.00800\ Residence\ time$$
$$* Mixing\ ratio + 0.012603\ Temperature^2$$
$$- 0.000386\ Residence\ time^2 + 0.0577677\ Mixing\ ratio$$

Considering the ANOVA analysis of the variables affecting the yield of hydrochar, temperature, and residence time were the most prevailing factors that affected the yield of hydrochar, both with p values < 0.0001. This is visualized in the response surface plot. The temperature had a downward trend with the yield of hydrochar. The highest yield of hydrochar (70.33%) occurred at 200 ℃, 60 min, and ratio 2. As the temperature was increased to 230, the yield of hydrochar decreased to 40.34%, 36.11%, and 32.69 at 60-, 90-, and 120-minute residence times, respectively. It shows that lower temperatures favour high hydrochar yield. Temperature's primary function is to provide heat for disintegration for the fragmentation of the biomass bond (Nizamuddin *et al.*, 2017). A more considerable percentage of the feedstock composition is putrefied when the carbonization temperature is increased which results in a reduction in the mass yield of the hydrochar. Hemicellulose, cellulose, and Lignin, in WH, were carbonized at HTC temperatures 180, 220, and 250 ℃, respectively. Hemicellulose is more unstable than cellulose and, as a result, degrades more easily into its monomers when heated. The hemicellulose monomers are xylose, mannose, glucose, and galactose. During the co-HTC process, xylose dissolves in the water as a pyranose ring which results in the formation of furfural (Tekin *et al.*, 2014). In a hydrothermal environment, as the density of water increases, so does hydrolysis, causing an increase in the decomposition of lignin to its low molecular weight components. Eventually, with the continual elevation of the reaction temperature to 250 °C, the lignin component of the biomass began hydrolysing, forming phenolic substances such as catechol and phenols.

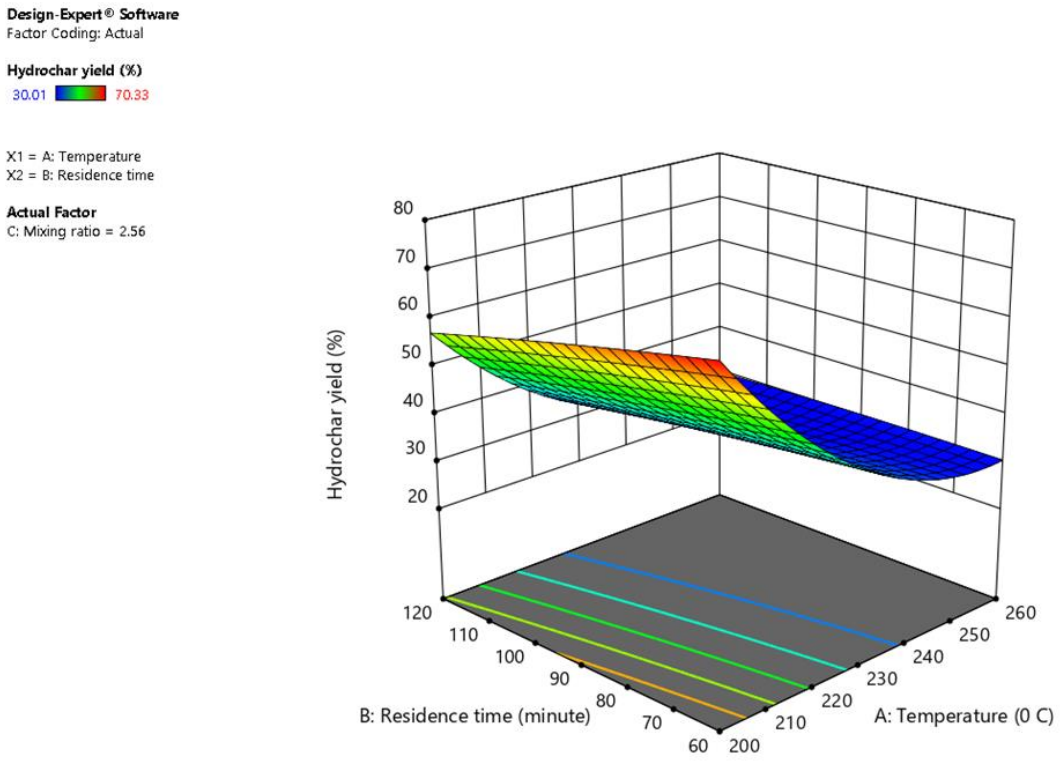

Figure 4.3 Response surface showing the effect of process parameters on hydrochar yield.

4.2.3 Effect of Process Parameters on High Heating Value.

For consideration as a fuel, the heating values of hydrochar are an important parameter. A high heating value indicates a high carbon content and the removal of volatile matter. The HHV was increased from 16.16 MJ/kg at 200 60 2 to 32.34 MJ/kg. This is an enhancement of the raw feedstocks which have HHV of 11.2 MJ/Kg and 13.4 MJ/Kg for PVC and WH respectively. The ANOVA table shows that increasing temperatures and resident time had a positive influence on the HHV of the hydrochar produced with p-values of <0.0001. The model that describes the relationship between the actual parameters and the HHV is given as:

$$High\ heating\ values$$
$$= -169.41704 + 1.43745 Temperature + 0.202189\ Residence\ time - 2.06156\ Mixing\ ratio - 0.000652\ Temperature * Residence\ time + 0.006594\ Temperature * Mixing\ ratio - 0.001562\ Residence\ time * Mixing\ ratio - 0.002596\ Temperature\text{^}2 + 0.000011\ Residence\ time\text{^}2 - 0.025188\ Mixing\ ratio\text{^}2$$

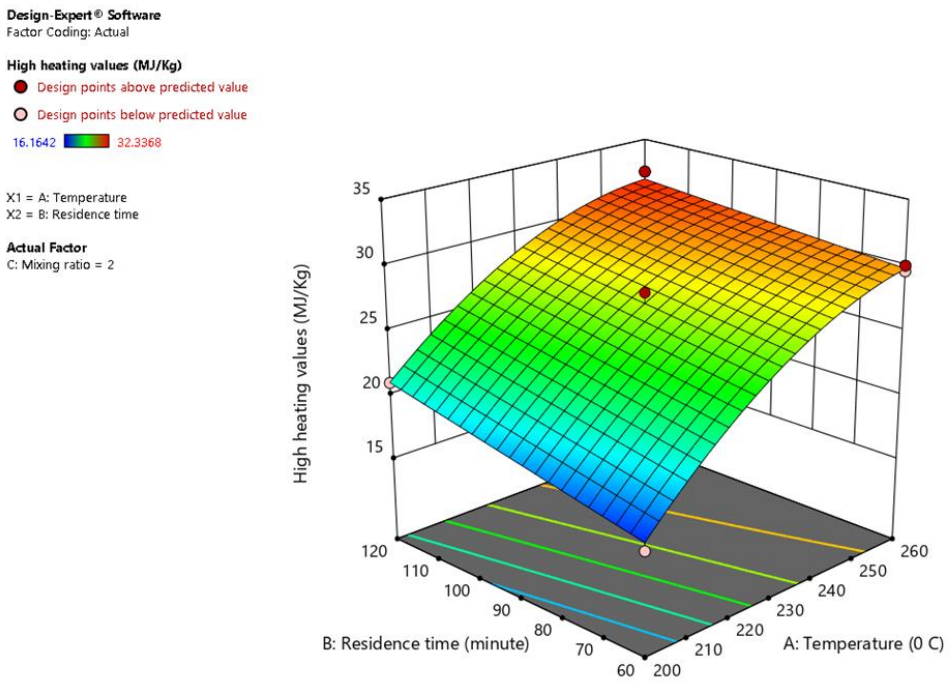

Figure 4.4 Response surface showing the effect of process parameters on High Heating Value.

4.3 FTIR Analysis

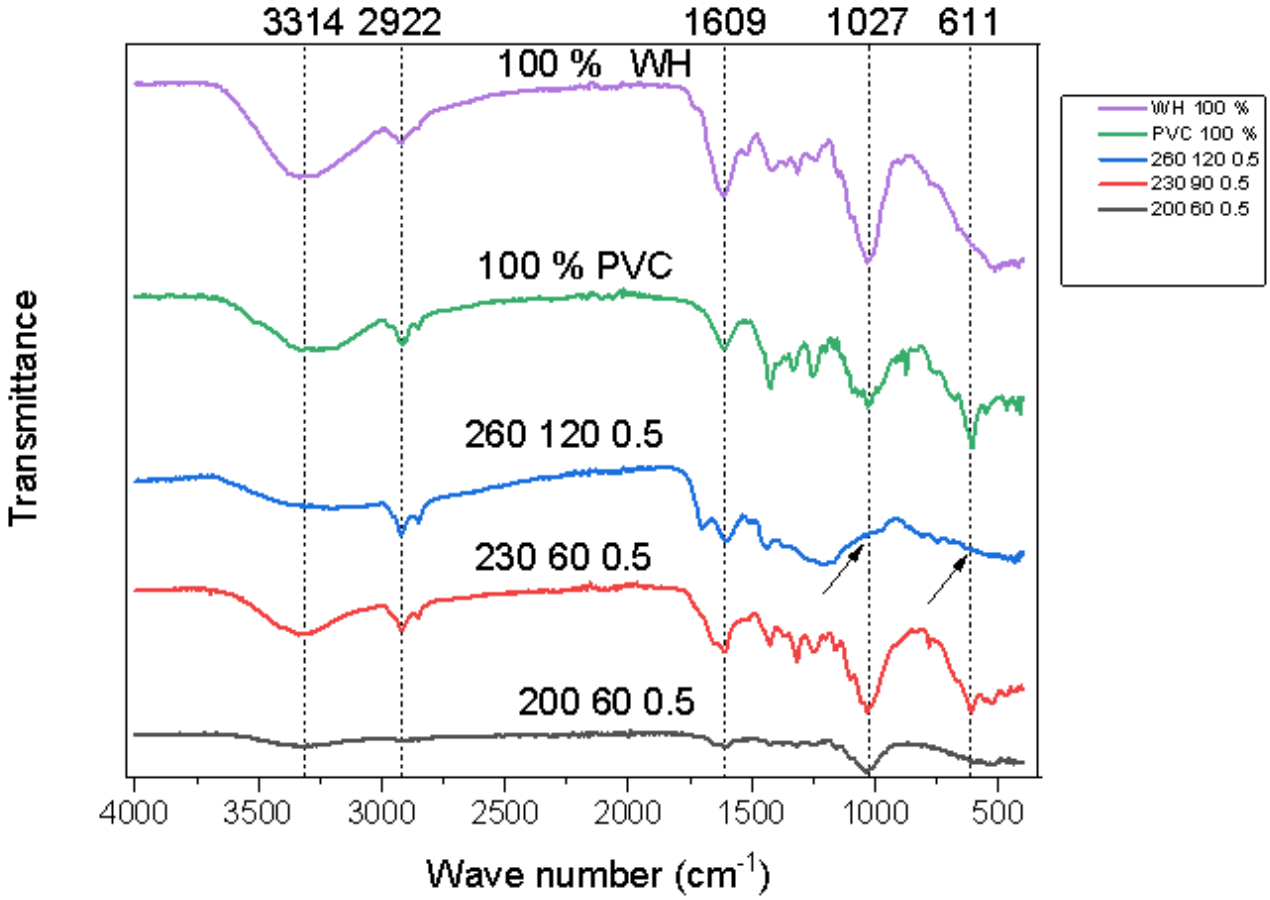

Figure 4.5 FT-IR graph for PVC, WH, and Hydrochar produced at 200 ℃, 230 ℃, and 260 ℃.

Fourier Transform Infrared Radioscopy (FTIR) analysis was used to investigate the chemical functional groups present in the hydrochar at various temperatures as well as the feedstock (PVC and WH) to better comprehend the chemical changes that transpire during co-HTC. Figure 4.5 shows the FTIR spectrum of the hydrochar and feedstocks. As shown in Figure 4.5, the FTIR spectra of untreated WH and PVC exhibit distinct features, showing that the two raw materials were characterized by different chemical compounds. The adsorption peak that occurred between 600 and 900 cm-1 for untreated PVC can be attributed to C-Cl stretching in alkyl halide groups of PVC chains (Wei *et al.*, 2022). The other peaks happening at 931 cm^{-1}, 950-1200 cm^{-1}, 1252 cm^{-1}, 1400-1700 cm^{-1}, and 2800-3000 cm^{-1},

were assigned to the vibrations of trans-CH wiggling, C-H stretching, CH_2 deformation, C=O in aromatic groups, and sp^3 C-H stretching in CH_n groups, respectively. The 1700 cm^{-1} band presented a C—O group in carbonyl, quinine, ester, or carboxyl residual on the surface of the dried water hyacinth and the hydrochar samples (Laginhas *et al*., 2016).

The bands at 1331–1254 cm−1 and 760–505 cm−1 were attributed to the presence of ─C─H and ─C─Cl (in the form of ─CHCl─) in PVC chains (Yao & Ma, 2018). It was visible that these bands in hydrochar were removed at 260 ℃, 120 min, and ratio of 0.5, indicating an excellent temperature dechlorinating effect of co-HTC via substitution and elimination reactions.

4.4 Thermographic Analysis

Thermal gravimetric analysis (TGA) evaluates weight changes in a substance under temperature control in a controlled environment. The decomposition behaviour of the biomass was assessed using a thermogravimetry analyser (TGA). TGA was conducted using 10 mL/min of air and a heating rate of 10 °C/min. The thermogravimetry (TG) and differential thermogravimetry (DTG) curves in Fig. 4.6 depict the thermal degradation characteristics of the feedstock and hydrochar. The decomposing profile of the PVC, WH, and hydrochar obtained at 200, 230, and 260 ℃ are displayed in Figure 4.7. The combustion of the PVC occurred in three main stages. The first stage occurred in the temperature range of 280 – 400 ℃. This combustion profile is because of the oxidation of light volatile matter in the PVC (Zhang *et al*., 2020). These materials include addictive and thickeners that were added to the PVC during synthesis. These materials burn at lower temperatures and are therefore liberated in the first combustion stage. The second stage of combustion occurred at the temperature range of 420-520 ℃. This is due to the oxidation of heavy volatile matter in the PVC. The liberation of some fixed carbon occurred within 550 – 600 ℃.

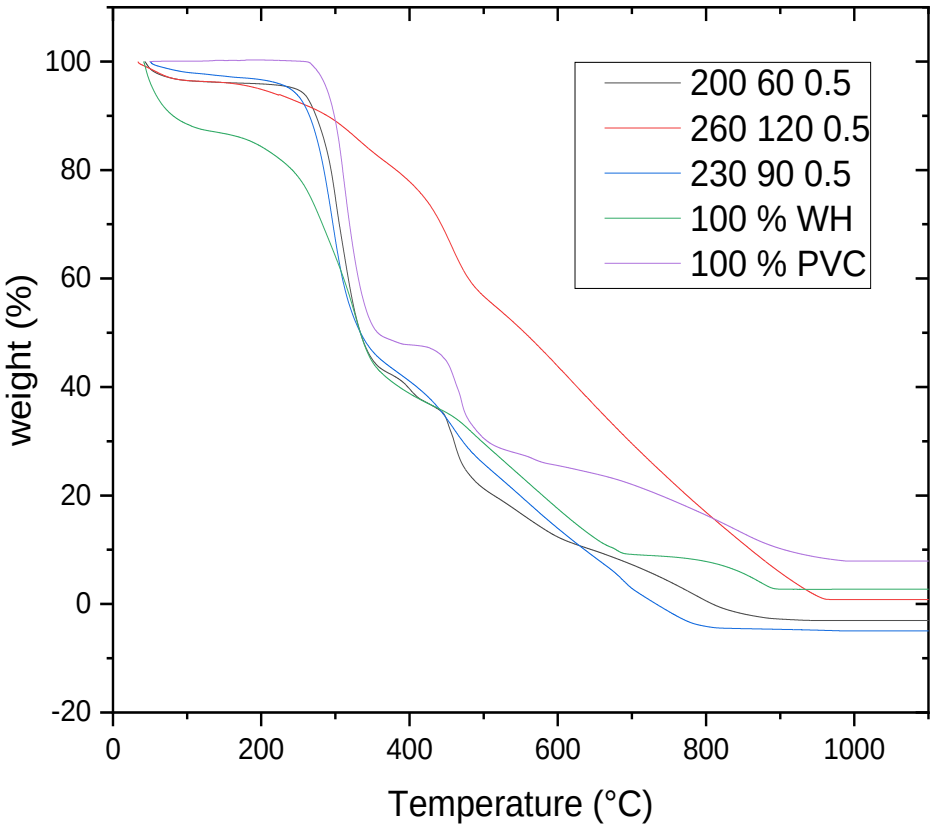

Figure 4.6. TGA graph showing the thermal decomposition of raw PVC and WH, and the hydrochars obtained at 200 ℃, 230 ℃, and 260 ℃.

The combustion of WH preceded in three stages as indicated by the three prominent peaks in Figure 4.6. The first stage (25- 130 ℃) resulted from the removal of moisture and volatile matter from WH. The second combustion stage occurred at the temperature range of 160 – 400 ℃. This stage represents the decomposing of cellulose and hemicellulose. Much of the weight loss in HW occurred in this stage since cellulose and hemicellulose forms the major component of WH. The degradation of lignin happened in the temperature series of 450 to 550 ℃. Char and inorganic formation from the WH occurred at temperatures beyond 600 ℃ (Gao *et al.*, 2013).

The TG and TGA curves that were obtained for the hydrochar were similar except for the hydrochar that was produced at the carbonization temperature of 260 ℃ which varies

slightly. The hydrochar had already been treated at lower temperatures which resulted in the removal of most volatile materials. As a result, lower peaks were registered at temperatures below 150 ℃. Three prominent peaks were registered for 200 ℃, 60 min, and ratio of 0.5. These peaks are at temperatures of 300 ℃, 400 ℃, and 460 ℃. The peak at 300 ℃ shows incomplete hydrolysis of cellulose and hemicellulose at a lower resident time and a faster decomposition at a lower temperature. *(*Gao *et al.*, 2013)

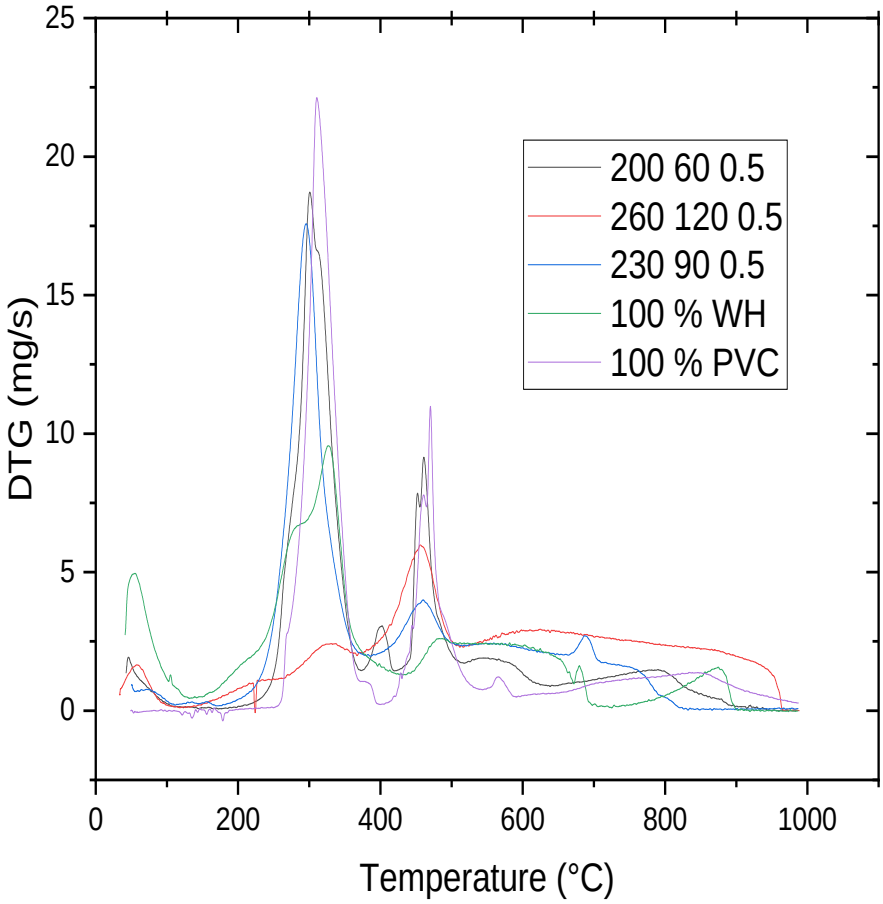

Figure 4.7. DTG graph showing peaks of elimination.

Co-dehydration hydrochars peaks were weaker than that of PVC and raw WH. Furthermore, it weakened with HTC temperature, indicating that the co-HTC process could effectively

remove inherent moisture from biomass and inhibit moisture re-adsorption. (Zhao *et al.*, 2021)

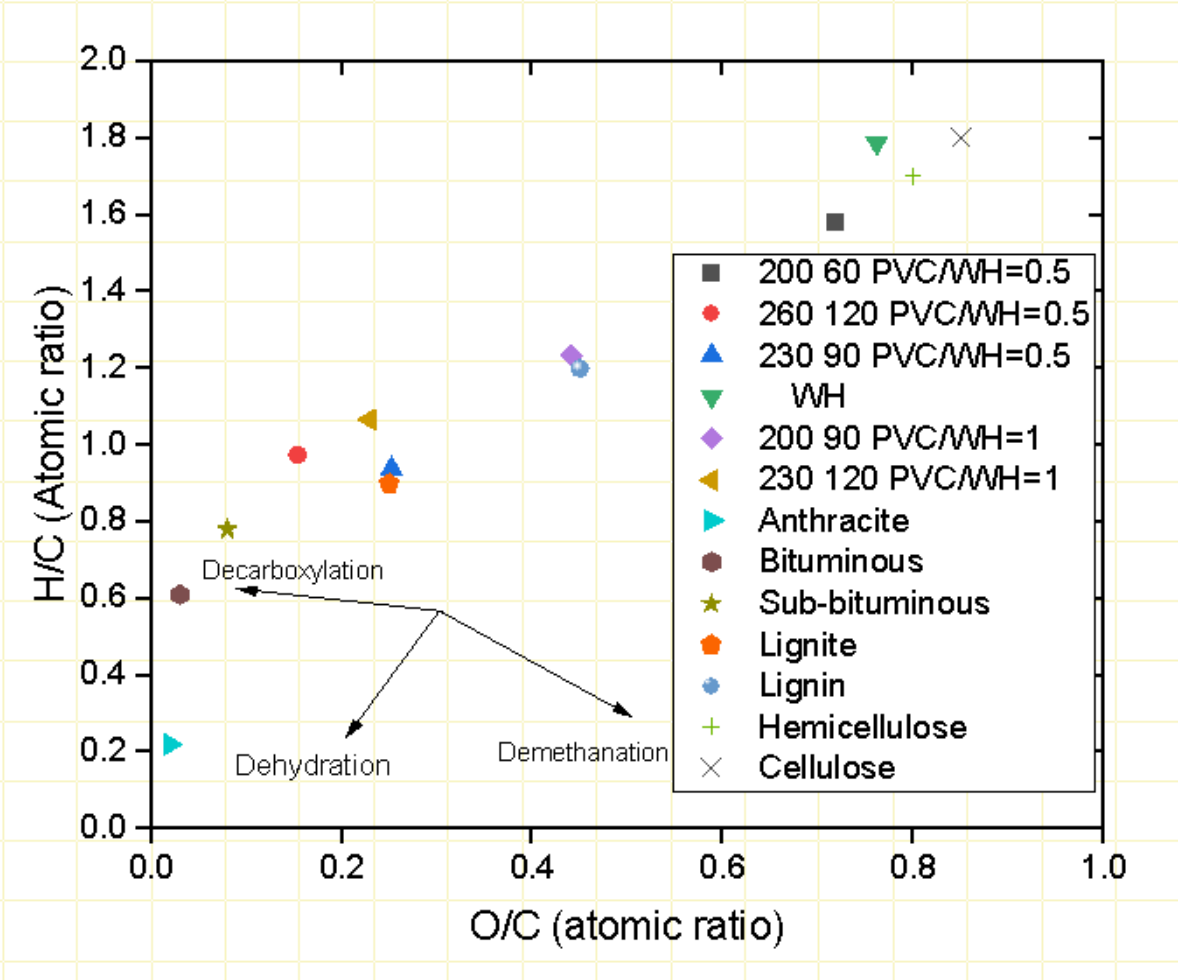

Figure 4.8. Van Krevelen diagram

The H/C and O/C ratios are significant conditions to evaluate the degree of deoxygenation, and the aromatic content during HTC of biomass (Tekin *et al.*, 2014) The raw feedstock and hydrochar H/C and O/C atomic ratios were displayed on the Van Krevelen diagram, as illustrated in Figure 4.8. The findings suggest that dehydration is the primary process of coalification of the feedstock, with the O/C and H/C atomic ratios falling with increasing temperature and residence time, and the fuel approaching more lignite in nature. The carbon content of hydrochar rose after the hydrothermal process, but the oxygen level fell significantly. Decarboxylation, dehydration, and demethanation reactions were implicated in the reaction pathways. (X. Zhang *et al.*, 2019) The energy densification of hydrochar

appears to be caused by changes in the carbon/oxygen (O/C) ratio in the fuel, with the carbon content appearing to grow while the oxygen and ash content appears to decrease. As a result, dehydration was an important response route.

4.5. Physical Characteristics of Hydrochar and Process Water

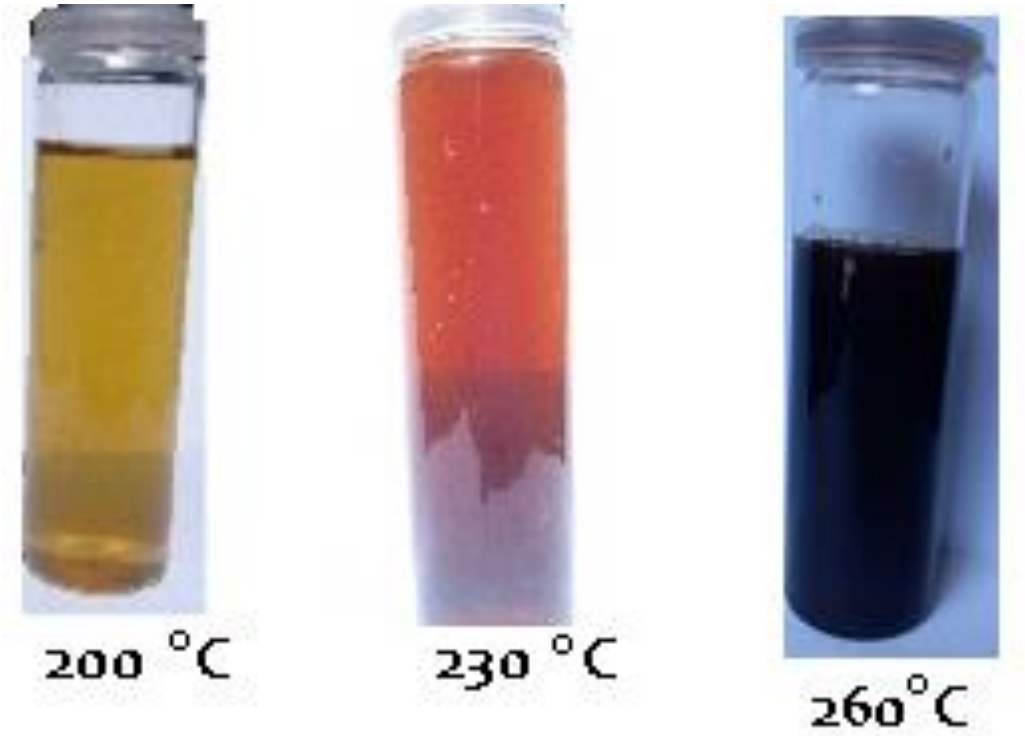

Figure 4.9. Colour changes in process water over temperature changes

The pH and electrical conductivity (EC) of the feedwater/process water were recorded with a pH meter. The results show a decline in the pH of the process water and an increase in their corresponding E.C. Organic acid formation are important intermediates in the HTC process to catalyse the disintegration of biomacromolecules and hydrochar formation (T. Wang *et al.*, 2018). The increase in pH is the result of the formation of formic, acetic, lactic, and levulinic acid from biomass.

The colour change of the process water also confirmed the changes in the chemical composition of the WH and PVC. Temperature increases result in the breaking of the bonds in the chemical structure of PVC and the biomass resulting in the release of free radicals into

the water which serves as the solvent. Therefore, the cleavage of the bonds depended heavily on the temperature, making the process water becoming darker as the temperature increased.

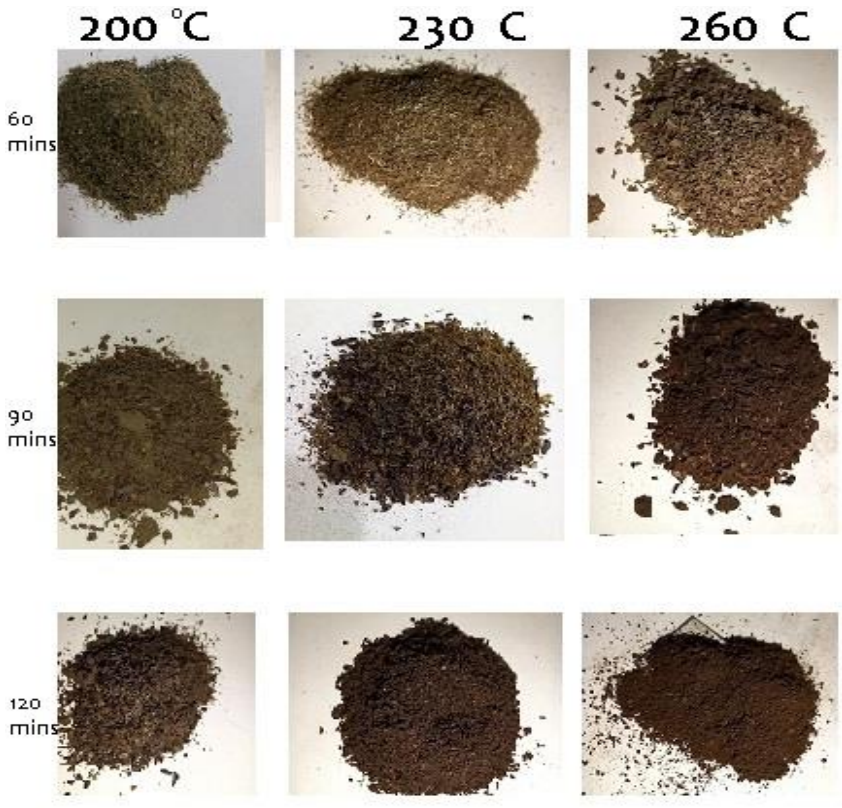

Figure 4.9.2. Sample of hydrochar produced at different temperatures, resident times, and mixing ratios.

CHAPTER FIVE

CONCLUSIONS AND RECOMMENDATION

5.1 Conclusion

The aim of this study centred on the optimization of the process parameters to produce hydrochar from waste PVC containing material and water hyacinth. Besides being a good source of energy, producing hydrochar from PVC and WH provided a safer means for disposing of halogenated waste through co-hydrothermal carbonization (Co-HTC) without releasing poisonous gases into the atmosphere. Blending the two feedstocks created a favourable medium(acidic) that aided the reaction.

The main factors that affected the yield of the solid fuel produced by Co-HTC were temperature and residence time. The mixing ratios of the feedstocks had a minimal impact on the yield. Even though a high yield of solid fuel was produced at lower temperatures (180 0 C), fuels produced at higher temperatures had high heating values and better combustion characteristics. At high temperatures, most of the volatile and inorganic matter that interfere with burning leading to the production of particulate matter which is undesirable in incinerators was drastically reduced.

High temperatures favoured the removal of inorganic chlorine from the PVC. The highest dechlorination efficiency, 94.39% was recorded at a high Co-HTC temperature of 260 ℃. The chlorine liberated from the PVC structure cleaved with free hydronium ions (+H) that were produced from the ionic dissociation of water molecules, to form hydrochloric acid (HCl). The HCl is soluble in water and remained in the filtrate when the resulting mixtures were filtered and washed.

According to the Fourier Transform Infrared (FT-IR) microscopy, the reactions that ensued in the Co-HTC process were hydrolysis, dehydration and decarboxylation, condensation and polymerization, and aromatization. These results show that temperature played a major role in the coalification of the feedstocks into useful fuels. These results were also confirmed by the reduction in the H/C and O/C ratios when the temperatures of the process were increased.

The thermogravimetric analysis of the solid fuel produced at various temperatures showed that the thermal properties of the fuels were enhanced as the temperatures of the reaction

were increased. As the inorganics and volatile matter were removed from the fuel, the intensities of the peaks were significantly reduced, with some vanishing completely which showed the elimination of specific inorganic material (especially Chlorine).

5.2 Recommendation

The following are some important recommendations:

- The reaction path for hydrothermal carbonization is not fully understood. This has hindered the effort to know the intermediary products that are formed during the reaction. These products when known and maximized may lead to the discovery of useful products. I recommend that studies be done on the reaction stages involved in the hydrothermal carbonization of biomass.
- The mathematical models that are used to describe or predict reactions in hydrothermal carbonization reactions are usually specific to the type of biomass that was used during the reaction. There is a need to obtain a general model that can be used to fit data or describe HTC reactions regardless of the type of biomass.

REFERENCES

Ahmad, M., Rajapaksha, A. U., Lim, J. E., Zhang, M., Bolan, N., Mohan, D., Vithanage, M., Lee, S. S., & Ok, Y. S. (2014). Biochar as a sorbent for contaminant management in soil and water: A review. *Chemosphere*, *99*, 19–33. https://doi.org/10.1016/j.chemosphere.2013.10.071

Al-Salem, S. M., Antelava, A., Constantinou, A., Manos, G., & Dutta, A. (2017). A review on thermal and catalytic pyrolysis of plastic solid waste (PSW). *Journal of Environmental Management*, *197*(1408), 177–198. https://doi.org/10.1016/j.jenvman.2017.03.084

Anupam, K., Sharma, A. K., Lal, P. S., Dutta, S., & Maity, S. (2016). Preparation, characterization and optimization for upgrading Leucaena leucocephala bark to biochar fuel with high energy yielding. *Energy*, *106*, 743–756. https://doi.org/10.1016/j.energy.2016.03.100

Arellano, O., Flores, M., Guerra, J., Hidalgo, A., Rojas, D., & Strubinger, A. (2016). Hydrothermal carbonization of corncob and characterization of the obtained hydrochar. *Chemical Engineering Transactions*, *50*(ii), 235–240. https://doi.org/10.3303/CET1650040

Azaare, L., Kweku, M., Mark, A., & Kemausuor, F. (2021). Bioresource Technology Reports Co-hydrothermal carbonization of pineapple and watermelon peels : Effects of process parameters on hydrochar yield and energy content. *Bioresource Technology Reports*, *15*(May), 100720. https://doi.org/10.1016/j.biteb.2021.100720

Bardhan, M., Mamun, T., Tabassum, M., Islam, A., Islam, A., & Hameed, B. H. (2021). Co-hydrothermal carbonization of different feedstocks to hydrochar as potential energy for the future world : A review. *Journal of Cleaner Production*, *298*, 126734. https://doi.org/10.1016/j.jclepro.2021.126734

Bobleter, O. (1994). Hydrothermal degradation of polymers derived from plants. *Progress in Polymer Science*, *19*(5), 797–841. https://doi.org/10.1016/0079-6700(94)90033-7

Bote, M. A., Naik, V. R., & Jagadeeshgouda, K. B. (2020). Materials Science for Energy Technologies Review on water hyacinth weed as a potential bio fuel crop to meet collective energy needs. *Materials Science for Energy Technologies*, *3*, 397–406. https://doi.org/10.1016/j.mset.2020.02.003

Cavali, M., Libardi, N., Dutra, J., Sena, D., Lorenci, A., Ricardo, C., Belli, P., Bayard, R., Benbelkacem, H., Borges, A., & Junior, D. C. (2023). Science of the Total Environment A review on hydrothermal carbonization of potential biomass wastes , characterization and environmental applications of hydrochar , and biore fi nery perspectives of the process. *Science of the Total Environment*, *857*(July 2022), 159627. https://doi.org/10.1016/j.scitotenv.2022.159627

Creamer, A. E., & Gao, B. (2016). Carbon-based adsorbents for postcombustion CO2 capture: A critical review. *Environmental Science and Technology*, *50*(14), 7276–7289. https://doi.org/10.1021/acs.est.6b00627

Das, S. P., Gupta, A., Das, D., & Goyal, A. (2016). Enhanced bioethanol production from water hyacinth (Eichhornia crassipes) by statistical optimization of fermentation process parameters using Taguchi orthogonal array design. *International Biodeterioration and Biodegradation*, *109*, 174–184. https://doi.org/10.1016/j.ibiod.2016.01.008

Demir-Cakan, R., Baccile, N., Antonietti, M., & Titirici, M. M. (2009). Carboxylate-rich carbonaceous materials via one-step hydrothermal carbonization of glucose in the presence of acrylic acid. *Chemistry of Materials*, *21*(3), 484–490. https://doi.org/10.1021/cm802141h

Du, B., Yu, Z., Tian, Y., & Ma, X. (2021). Effects of baking soda on Co-hydrothermal carbonization of sewage sludge and Chlorella vulgaris: Improved the environmental friendliness of hydrochar incineration process. *Journal of Environmental Chemical Engineering*, *9*(6), 106404. https://doi.org/10.1016/j.jece.2021.106404

Fiori, L., Basso, D., Castello, D., & Baratieri, M. (2014). Hydrothermal carbonization of biomass: Design of a batch reactor and preliminary experimental results. *Chemical Engineering Transactions*, *37*, 55–60. https://doi.org/10.3303/CET1437010

Gao, Y., Wang, X., Wang, J., Li, X., Cheng, J., Yang, H., & Chen, H. (2013). Effect of residence time on chemical and structural properties of hydrochar obtained by hydrothermal carbonization of water hyacinth. *Energy*, *58*, 376–383. https://doi.org/10.1016/j.energy.2013.06.023

Heidari, M., Dutta, A., Acharya, B., & Mahmud, S. (2019). A review of the current knowledge and challenges of hydrothermal carbonization for biomass conversion. *Journal of the Energy Institute*, *92*(6), 1779–1799. https://doi.org/10.1016/j.joei.2018.12.003

Hosokai, S., Matsuoka, K., Kuramoto, K., & Suzuki, Y. (2016). Modification of Dulong's formula to estimate heating value of gas, liquid and solid fuels. *Fuel Processing Technology*, *152*, 399–405. https://doi.org/10.1016/j.fuproc.2016.06.040

Hu, Y., Zhang, Q., Hu, S., Xiao, G., Chen, X., & Wang, J. (2022). Research progress and prospects of ecosystem carbon sequestration under climate change (1992 – 2022). *Ecological Indicators*, *145*(July), 109656. https://doi.org/10.1016/j.ecolind.2022.109656

Huang, N., Zhao, P., Ghosh, S., & Fedyukhin, A. (2019a). Co-hydrothermal carbonization of polyvinyl chloride and moist biomass to remove chlorine and inorganics for clean fuel production. *Applied Energy*, *240*(February), 882–892. https://doi.org/10.1016/j.apenergy.2019.02.050

Huang, N., Zhao, P., Ghosh, S., & Fedyukhin, A. (2019b). Co-hydrothermal carbonization of polyvinyl chloride and moist biomass to remove chlorine and inorganics for clean fuel production. *Applied Energy*, *240*(October 2018), 882–892. https://doi.org/10.1016/j.apenergy.2019.02.050

International Biochar Initiative. (2015). Standardized Product Definition and Product Testing Guidelines for Biochar That Is Used in Soil. *International Biochar Initiative*, *November*, 23. http://www.biochar-international.org/sites/default/files/Guidelines_for_Biochar_That_Is_Used_in_Soil_Final.pdf

Kambo, H. S., & Dutta, A. (2015). A comparative review of biochar and hydrochar in terms of production, physico-chemical properties and applications. *Renewable and Sustainable Energy Reviews*, *45*, 359–378. https://doi.org/10.1016/j.rser.2015.01.050

Kaur, M., Kumar, M., Sachdeva, S., & Puri, S. K. (2018). Aquatic weeds as the next generation feedstock for sustainable bioenergy production. *Bioresource Technology*, *251*(October 2017), 390–402. https://doi.org/10.1016/j.biortech.2017.11.082

Khan, T. A., Saud, A. S., Jamari, S. S., Rahim, M. H. A., Park, J. W., & Kim, H. J. (2019). Hydrothermal carbonization of lignocellulosic biomass for carbon rich material preparation: A review. *Biomass and Bioenergy*, *130*(August), 105384. https://doi.org/10.1016/j.biombioe.2019.105384

Laginhas, C., Nabais, J. M. V., & Titirici, M. M. (2016). Activated carbons with high nitrogen content by a combination of hydrothermal carbonization with activation. *Microporous and Mesoporous Materials*, *226*, 125–132. https://doi.org/10.1016/j.micromeso.2015.12.047

Lee, J., Sohn, D., Lee, K., & Park, K. Y. (2019). Solid fuel production through hydrothermal carbonization of sewage sludge and microalgae Chlorella sp. from wastewater treatment plant. *Chemosphere*, *230*, 157–163. https://doi.org/10.1016/j.chemosphere.2019.05.066

Libra, J. A., Ro, K. S., Kammann, C., Funke, A., Berge, N. D., Neubauer, Y., Titirici, M. M., Fühner, C., Bens, O., Kern, J., & Emmerich, K. H. (2011). Hydrothermal carbonization of biomass residuals: A comparative review of the chemistry, processes and applications of wet and dry pyrolysis. *Biofuels*, *2*(1), 71–106. https://doi.org/10.4155/bfs.10.81

Liu, Z., Quek, A., Kent Hoekman, S., & Balasubramanian, R. (2013). Production of solid biochar fuel from waste biomass by hydrothermal carbonization. *Fuel*, *103*, 943–949. https://doi.org/10.1016/j.fuel.2012.07.069

Lu, X., Ma, X., Chen, X., Yao, Z., & Zhang, C. (2020). Bioresource Technology Co-hydrothermal carbonization of polyvinyl chloride and corncob for clean solid fuel

production. *Bioresource Technology*, *301*(November 2019), 122763. https://doi.org/10.1016/j.biortech.2020.122763

Lu, X., Ma, X., Qin, Z., Chen, X., Chen, L., & Tian, Y. (2021). Journal of Environmental Chemical Engineering Co-hydrothermal carbonization of sewage sludge and polyvinyl chloride : Hydrochar properties and fate of chlorine and heavy metals. *Journal of Environmental Chemical Engineering*, *9*(5), 106143. https://doi.org/10.1016/j.jece.2021.106143

Lynam, J. G., Toufiq Reza, M., Vasquez, V. R., & Coronella, C. J. (2012). Effect of salt addition on hydrothermal carbonization of lignocellulosic biomass. *Fuel*, *99*, 271–273. https://doi.org/10.1016/j.fuel.2012.04.035

Ma, D., Feng, Q., Chen, B., Cheng, X., Chen, K., & Li, J. (2019). Insight into chlorine evolution during hydrothermal carbonization of medical waste model. *Journal of Hazardous Materials*, *380*(100), 120847. https://doi.org/10.1016/j.jhazmat.2019.120847

Marcus, Y. (1999). On transport properties of hot liquid and supercritical water and their relationship to the hydrogen bonding. *Fluid Phase Equilibria*, *164*(1), 131–142. https://doi.org/10.1016/S0378-3812(99)00244-7

Matus, C., Camú, E., Villarroel, M., Ojeda, J., & Baeza, P. (2016). Study of the removal of 4-Nitrophenol from aqueous media by adsorption on different materials. *Journal of the Chilean Chemical Society*, *61*(2), 2898–2902. https://doi.org/10.4067/S0717-97072016000200010

Ning, X., Dang, H., Xu, R., Wang, G., Zhang, J., Zhang, N., & Wang, C. (2022a). Co-hydrothermal carbonization of biomass and PVC for clean blast furnace injection fuel production : Experiment and DFT calculation. *Renewable Energy*, *187*, 156–168. https://doi.org/10.1016/j.renene.2022.01.082

Ning, X., Dang, H., Xu, R., Wang, G., Zhang, J., Zhang, N., & Wang, C. (2022b). Co-hydrothermal carbonization of biomass and PVC for clean blast furnace injection fuel production: Experiment and DFT calculation. *Renewable Energy*, *187*, 156–168.

https://doi.org/10.1016/j.renene.2022.01.082

Nizamuddin, S., Baloch, H. A., Griffin, G. J., Mubarak, N. M., Bhutto, A. W., Abro, R., Mazari, S. A., & Ali, B. S. (2017). An overview of effect of process parameters on hydrothermal carbonization of biomass. *Renewable and Sustainable Energy Reviews*, *73*(December 2015), 1289–1299. https://doi.org/10.1016/j.rser.2016.12.122

Pattra, S., & Sittijunda, S. (2015). Optimization of Factors Affecting Acid Hydrolysis of Water Hyacinth Stem (Eichhornia Crassipes) for Bio-Hydrogen Production. In *Energy Procedia* (Vol. 79). Elsevier B.V. https://doi.org/10.1016/j.egypro.2015.11.574

Pauline, A. L., & Joseph, K. (2020). Hydrothermal carbonization of organic wastes to carbonaceous solid fuel – A review of mechanisms and process parameters. *Fuel*, *279*(April), 118472. https://doi.org/10.1016/j.fuel.2020.118472

Plastics – the Facts 2020. (2020).

Poerschmann, J., Weiner, B., Woszidlo, S., Koehler, R., & Kopinke, F. (2015a). Chemosphere Hydrothermal carbonization of poly (vinyl chloride). *Chemosphere*, *119*, 682–689. https://doi.org/10.1016/j.chemosphere.2014.07.058

Poerschmann, J., Weiner, B., Woszidlo, S., Koehler, R., & Kopinke, F. D. (2015b). Hydrothermal carbonization of poly(vinyl chloride). *Chemosphere*, *119*, 682–689. https://doi.org/10.1016/j.chemosphere.2014.07.058

Reza, M. T., Andert, J., Wirth, B., Busch, D., Pielert, J., Lynam, J. G., & Mumme, J. (2014). Hydrothermal Carbonization of Biomass for Energy and Crop Production. *Applied Bioenergy*, *1*(1), 11–29. https://doi.org/10.2478/apbi-2014-0001

Román, S., Ledesma, B., Álvarez, A., Coronella, C., & Qaramaleki, S. V. (2020). Suitability of hydrothermal carbonization to convert water hyacinth to added-value products. *Renewable Energy*, *146*, 1649–1658. https://doi.org/10.1016/j.renene.2019.07.157

Ruiz, H. A., Rodríguez-Jasso, R. M., Fernandes, B. D., Vicente, A. A., & Teixeira, J. A. (2013). Hydrothermal processing, as an alternative for upgrading agriculture residues

and marine biomass according to the biorefinery concept: A review. *Renewable and Sustainable Energy Reviews*, *21*, 35–51. https://doi.org/10.1016/j.rser.2012.11.069

Sahoo, D., Awasthi, A., Dhyani, V., Biswas, B., Kumar, J., Reddy, Y. S., Adarsh, V. P., Puthiyamadam, A., Mallapureddy, K. K., Sukumaran, R. K., Ummalyma, S. B., & Bhaskar, T. (2019). Value-addition of water hyacinth and para grass through pyrolysis and hydrothermal liquefaction. *Carbon Resources Conversion*, *2*(3), 233–241. https://doi.org/10.1016/j.crcon.2019.08.001

Sevilla, M., & Fuertes, A. B. (2009). The production of carbon materials by hydrothermal carbonization of cellulose. *Carbon*, *47*(9), 2281–2289. https://doi.org/10.1016/j.carbon.2009.04.026

Shen, Y. (2020a). A review on hydrothermal carbonization of biomass and plastic wastes to energy products. *Biomass and Bioenergy*, *134*(August 2019), 105479. https://doi.org/10.1016/j.biombioe.2020.105479

Shen, Y. (2020b). Biomass and Bioenergy A review on hydrothermal carbonization of biomass and plastic wastes to energy products. *Biomass and Bioenergy*, *134*(August 2019), 105479. https://doi.org/10.1016/j.biombioe.2020.105479

Tekin, K., & Karagöz, S. (2013). t-BuOK catalyzed bio-oil production from woody biomass under sub-critical water conditions. *Environmental Chemistry Letters*, *11*(1), 25–31. https://doi.org/10.1007/s10311-012-0373-3

Tekin, K., Karagöz, S., & Bektaş, S. (2014). A review of hydrothermal biomass processing. *Renewable and Sustainable Energy Reviews*, *40*, 673–687. https://doi.org/10.1016/j.rser.2014.07.216

Titirici, M. M., & Antonietti, M. (2010). Chemistry and materials options of sustainable carbon materials made by hydrothermal carbonization. *Chemical Society Reviews*, *39*(1), 103–116. https://doi.org/10.1039/b819318p

Tu, W., Liu, Y., Xie, Z., Chen, M., Ma, L., Du, G., & Zhu, M. (2021). A novel activation-hydrochar via hydrothermal carbonization and KOH activation of sewage sludge and coconut shell for biomass wastes: Preparation, characterization and adsorption

properties. *Journal of Colloid and Interface Science*, *593*, 390–407. https://doi.org/10.1016/j.jcis.2021.02.133

Vanavanichkul, T., Le, G. T. T., Lawagon, C. P., Sano, N., Viriya-empikul, N., Faungnawakij, K., & Charinpanitkul, T. (2021). Step-by-step conversion of water hyacinth waste to carbon nanohorns by a combination of hydrothermal treatment, carbonization and arc in water processes. *Diamond and Related Materials*, *111*(August 2020), 108222. https://doi.org/10.1016/j.diamond.2020.108222

Wang, L., Chang, Y., & Li, A. (2019). Hydrothermal carbonization for energy-efficient processing of sewage sludge: A review. *Renewable and Sustainable Energy Reviews*, *108*(April), 423–440. https://doi.org/10.1016/j.rser.2019.04.011

Wang, T., Zhai, Y., Zhu, Y., Li, C., & Zeng, G. (2018). A review of the hydrothermal carbonization of biomass waste for hydrochar formation: Process conditions, fundamentals, and physicochemical properties. *Renewable and Sustainable Energy Reviews*, *90*(February), 223–247. https://doi.org/10.1016/j.rser.2018.03.071

Wei, Y., Fakudze, S., Zhang, Y., Ma, R., & Shang, Q. (2022). *Co-hydrothermal carbonization of pomelo peel and PVC for production of hydrochar pellets with enhanced fuel properties and dechlorination*. *239*. https://doi.org/10.1016/j.energy.2021.122350

Wilk, M., Śliz, M., & Lubieniecki, B. (2021). Hydrothermal co-carbonization of sewage sludge and fuel additives: Combustion performance of hydrochar. *Renewable Energy*, *178*, 1046–1056. https://doi.org/10.1016/j.renene.2021.06.101

Xu, Z., Qi, R., Zhang, D., Gao, Y., Xiong, M., & Chen, W. (2021). Co-hydrothermal carbonization of cotton textile waste and polyvinyl chloride waste for the production of solid fuel : Interaction mechanisms and combustion behaviors. *Journal of Cleaner Production*, *316*(July), 128306. https://doi.org/10.1016/j.jclepro.2021.128306

Yadav, P., & Reddy, S. N. (2020). Bioresource Technology Hydrothermal liquefaction of Fe-impregnated water hyacinth for generation of liquid bio-fuels and nano Fe carbon hybrids. *Bioresource Technology*, *313*(May), 123691.

https://doi.org/10.1016/j.biortech.2020.123691

Yang, J., (Sophia)He, Q., & Yang, L. (2019). A review on hydrothermal co-liquefaction of biomass. *Applied Energy*, *250*(April), 926–945. https://doi.org/10.1016/j.apenergy.2019.05.033

Yao, Z., & Ma, X. (2018). Bioresource Technology Characteristics of co-hydrothermal carbonization on polyvinyl chloride wastes with bamboo. *Bioresource Technology*, *247*(381), 302–309. https://doi.org/10.1016/j.biortech.2017.09.098

Zhang, C., Ma, X., Huang, T., Zhou, Y., & Tian, Y. (2020). Co-hydrothermal carbonization of water hyacinth and polyvinyl chloride: Optimization of process parameters and characterization of hydrochar. *Bioresource Technology*, *314*(June), 123676. https://doi.org/10.1016/j.biortech.2020.123676

Zhang, C., Ma, X., Zheng, C., Huang, T., Lu, X., & Tian, Y. (2020). *Co-hydrothermal Carbonization of Water Hyacinth and Sewage Sludge : E ff ects of Aqueous Phase Recirculation on the Characteristics of Hydrochar*. https://doi.org/10.1021/acs.energyfuels.0c01991

Zhang, X., Zhang, L., & Li, A. (2019). Bioresource Technology Co-hydrothermal carbonization of lignocellulosic biomass and waste polyvinyl chloride for high-quality solid fuel production : Hydrochar properties and its combustion and pyrolysis behaviors. *Bioresource Technology*, *294*(June), 122113. https://doi.org/10.1016/j.biortech.2019.122113

Zhao, P., Huang, N., Li, J., & Cui, X. (2020). Fate of sodium and chlorine during the co-hydrothermal carbonization of high-alkali coal and polyvinyl chloride. *Fuel Processing Technology*, *199*(November 2019), 106277. https://doi.org/10.1016/j.fuproc.2019.106277

Zhao, P., Li, Z., Li, T., Yan, W., & Ge, S. (2017). The study of nickel effect on the hydrothermal dechlorination of PVC. *Journal of Cleaner Production*, *152*, 38–46. https://doi.org/10.1016/J.JCLEPRO.2017.03.101

Zhao, P., Lin, C., Zhang, J., Huang, N., Cui, X., Tian, H., & Guo, Q. (2021). Moisture re-

adsorption characteristics of hydrochar generated from the Co-hydrothermal carbonization of PVC and alkali coal. *Fuel Processing Technology*, *213*(October 2020), 106636. https://doi.org/10.1016/j.fuproc.2020.106636

APPENDIX

Appendix 1

The normal plot of data versus residuals for estimating errors

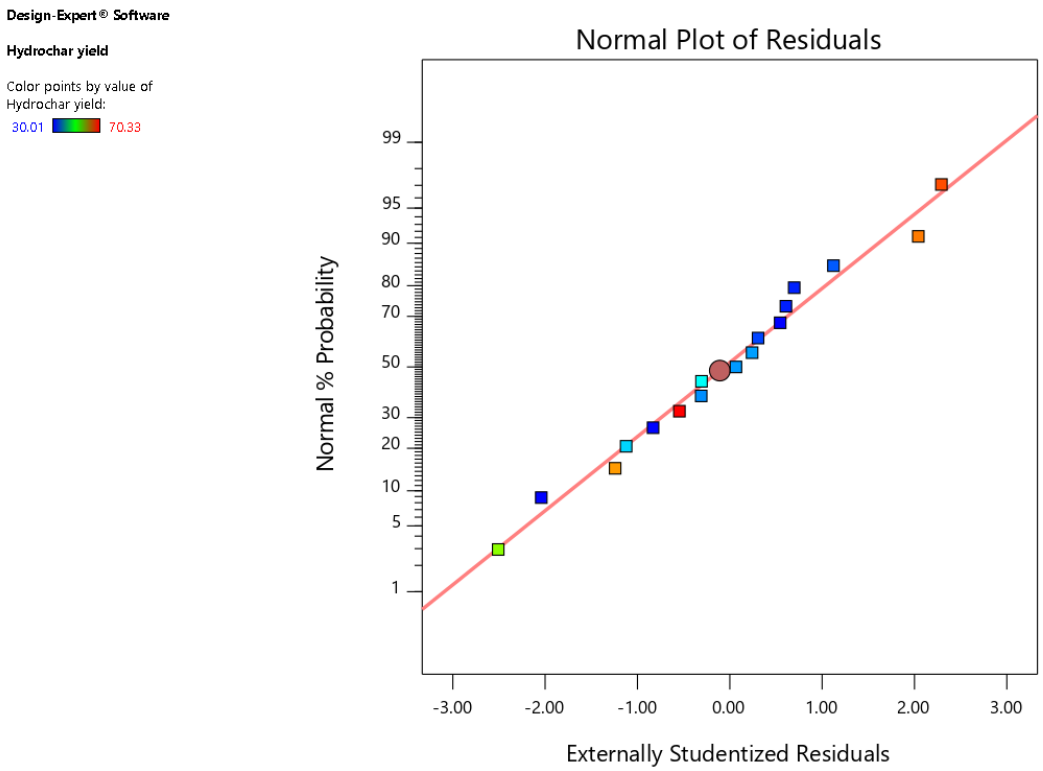

Appendix 2

Plot of Predicted values against Actual values

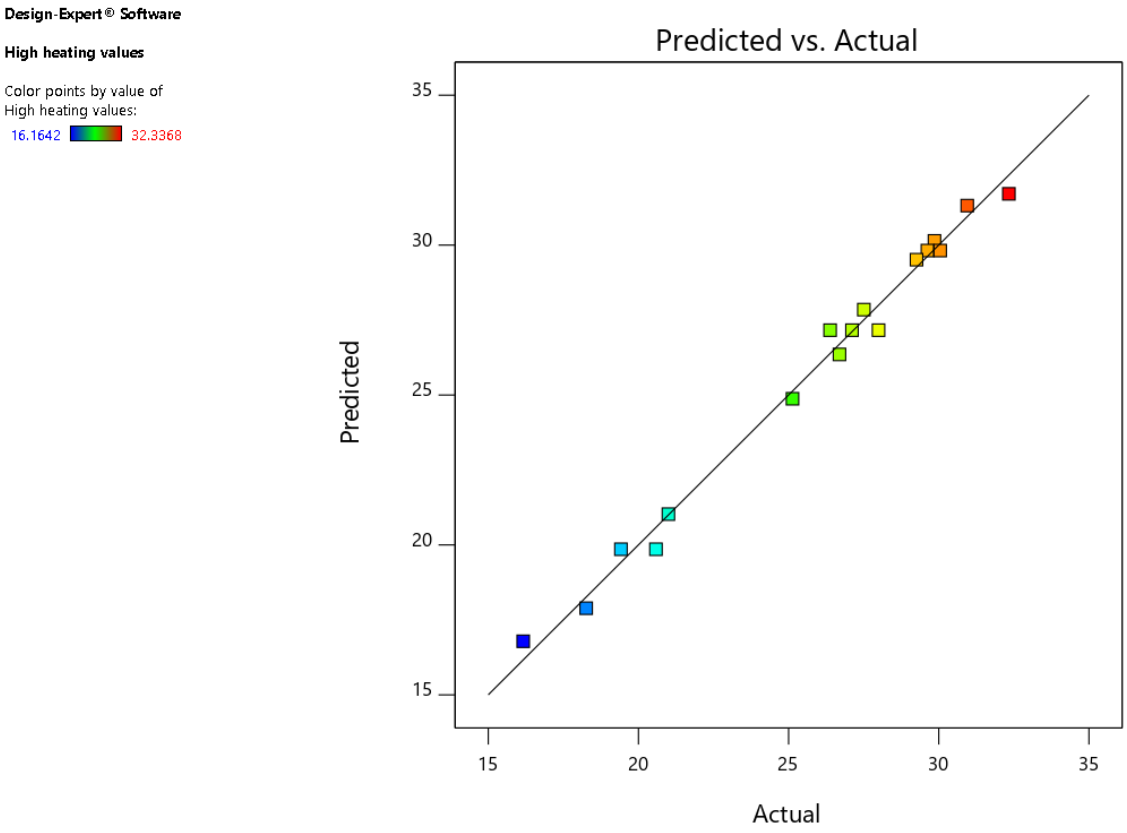

Appendix 3

Plot of Residuals values against Predicted value

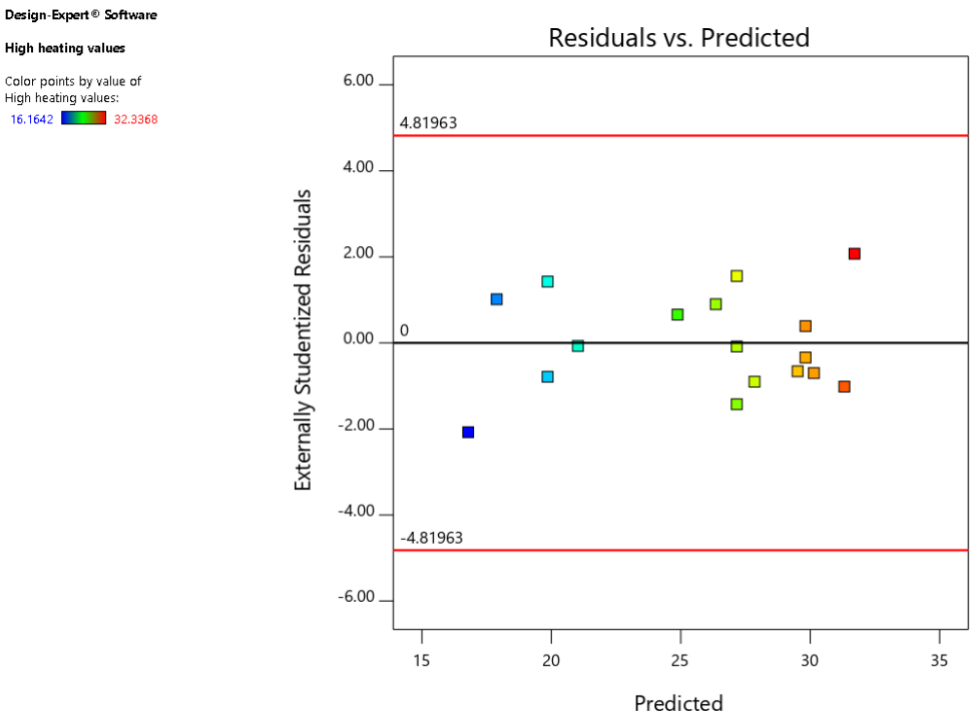

Appendix 4

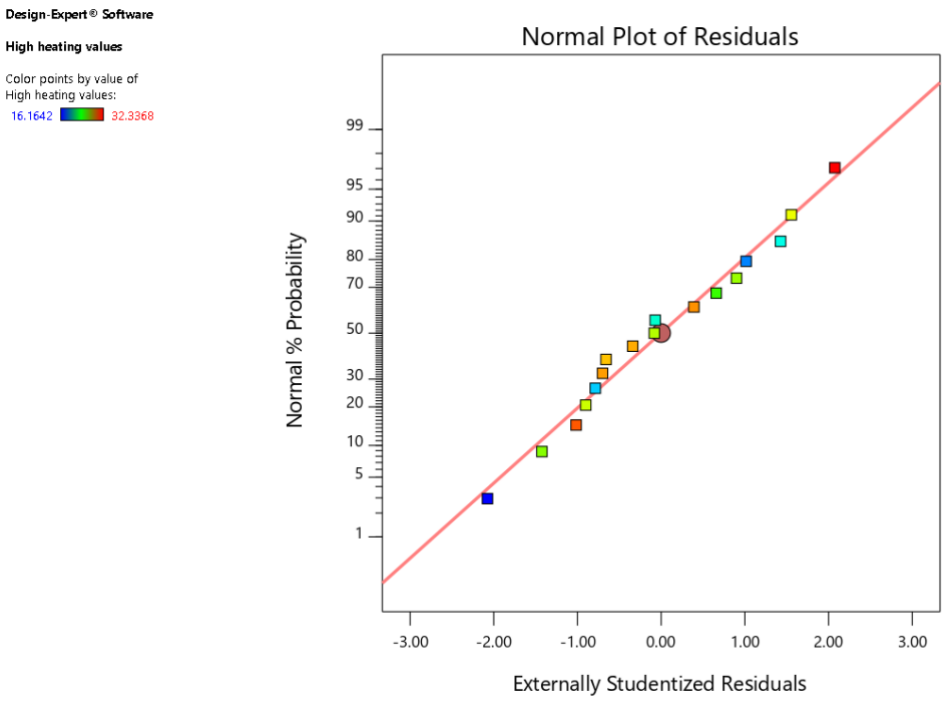

Appendix 5

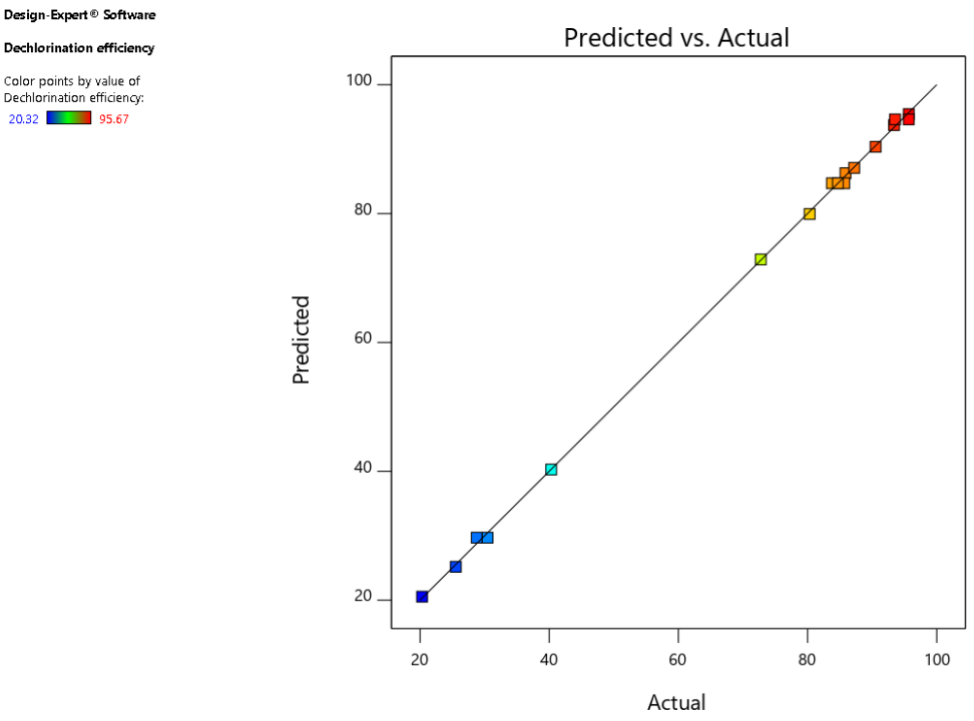

Appendix 6

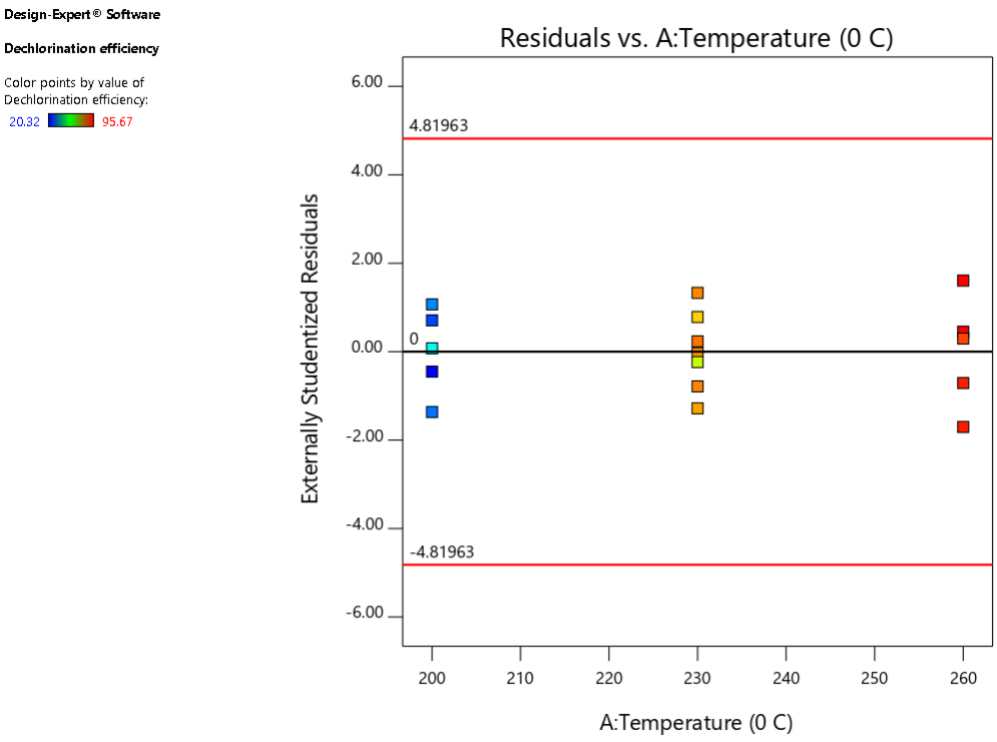

Appendix 7

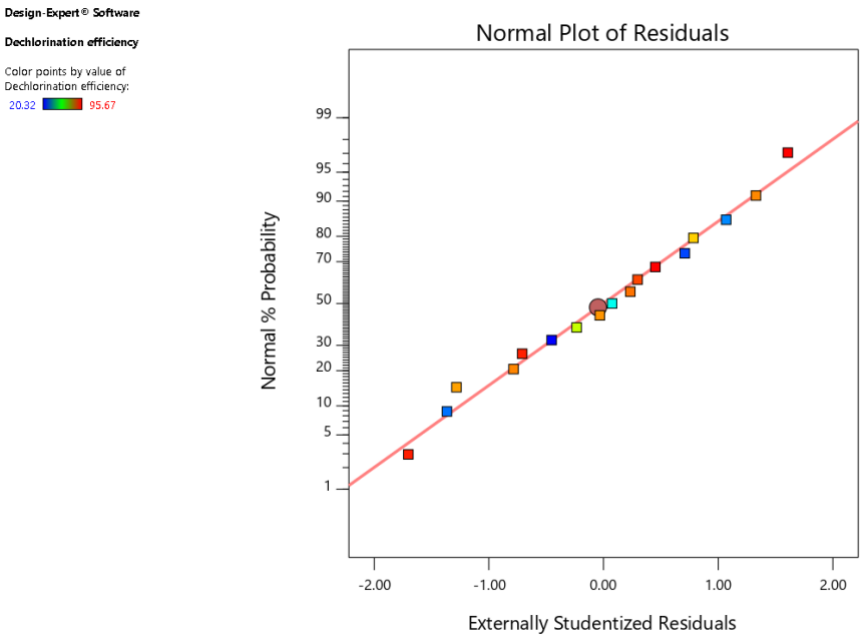

Appendix 8

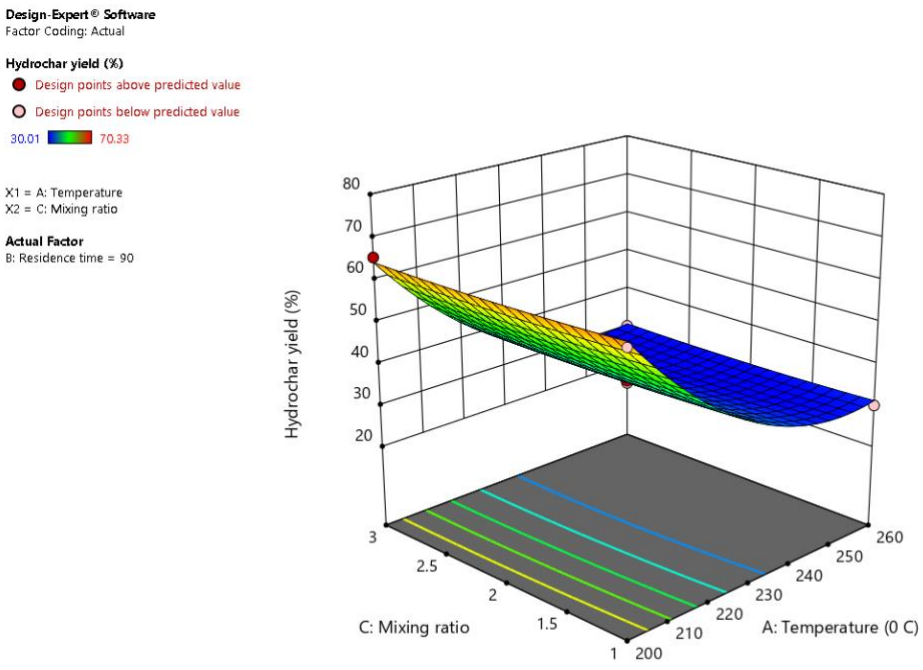

Appendix 9

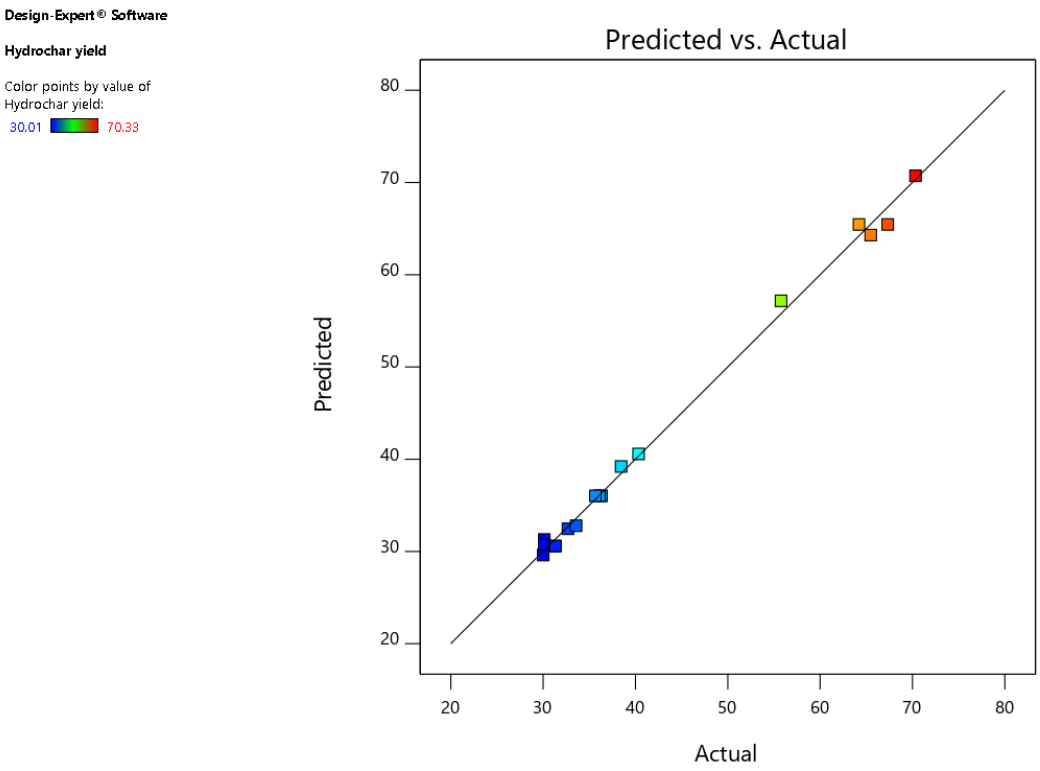
Design-Expert® Software
Hydrochar yield
Color points by value of
Hydrochar yield:
30.01
70.33
Predicted vs. Actual
Predicted
Actual
20
30
40
50
60
70
80

Appendix 10

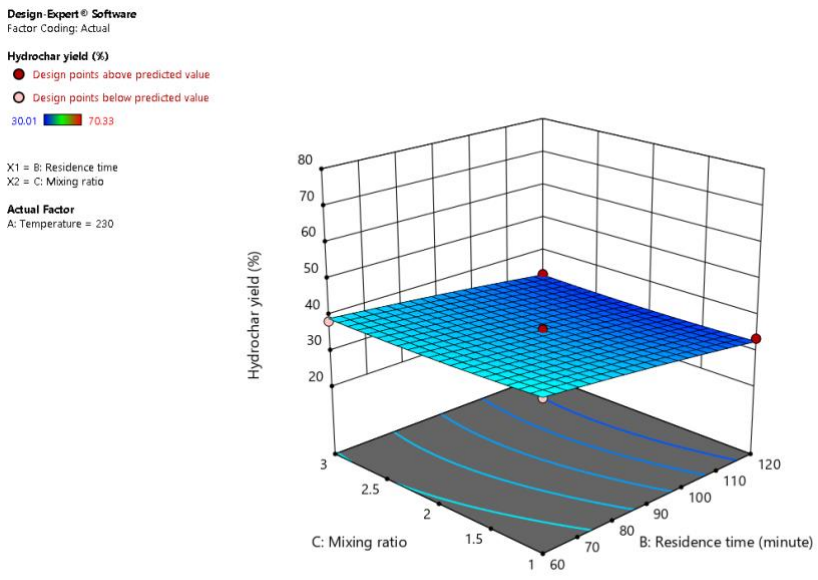
Design-Expert® Software
Factor Coding: Actual
Hydrochar yield (%)
Design points above predicted value
Design points below predicted value
30.01
70.33
X1 = B: Residence time
X2 = C: Mixing ratio
Actual Factor
A: Temperature = 230
Hydrochar yield (%)
C: Mixing ratio
B: Residence time (minute)

Appendix 11. Reaction Parameters and output variables of the process optimization experiments.

Source	Sum of Squares	df	Mean Square	F-value	p-value	
High heating values						
Model	378.42	9	42.05	81.37	< 0.0001	significant
A-Temperature	324.39	1	324.39	627.77	< 0.0001	
B-Residence time	20.25	1	20.25	39.19	0.0004	
C-Mixing ratio	5.33	1	5.33	10.31	0.0148	
AB	1.61	1	1.61	3.11	0.1211	
AC	0.1828	1	0.1828	0.3538	0.5707	
BC	0.0088	1	0.0088	0.0170	0.8999	
A^2	21.70	1	21.70	42.00	0.0003	
B^2	0.0004	1	0.0004	0.0007	0.9790	
C^2	0.0025	1	0.0025	0.0048	0.9465	
Residual	3.62	7	0.5167			
Lack of Fit	1.54	3	0.5141	0.9910	0.4821	not significant
Dechlorination Efficiency						
Model	12735.53	9	1415.06	1586.03	< 0.0001	significant
A-Temperature	9634.94	1	9634.94	10799.08	< 0.0001	
B-Residence time	227.38	1	227.38	254.86	< 0.0001	
C-Mixing ratio	33.48	1	33.48	37.53	0.0005	

AB	104.38	1	104.38	116.99	< 0.0001	
AC	0.3846	1	0.3846	0.4310	0.5325	
BC	9.67	1	9.67	10.84	0.0133	
A^2	1905.13	1	1905.13	2135.31	< 0.0001	
B^2	0.0399	1	0.0399	0.0447	0.8386	
C^2	37.11	1	37.11	41.59	0.0004	
Residual	6.25	7	0.8922			
Lack of Fit	0.7427	3	0.2476	0.1800	0.9048	not significant
Hydrochar Yield						
Model	3586.75	9	398.53	213.58	< 0.0001	significant
A-Temperature	2644.26	1	2644.26	1417.13	< 0.0001	
B-Residence time	113.88	1	113.88	61.03	0.0001	
C-Mixing ratio	1.54	1	1.54	0.8252	0.3939	
AB	46.20	1	46.20	24.76	0.0016	
AC	0.1056	1	0.1056	0.0566	0.8188	
BC	0.2601	1	0.2601	0.1394	0.7199	
A^2	511.35	1	511.35	274.05	< 0.0001	
B^2	0.4756	1	0.4756	0.2549	0.6292	
C^2	1.31	1	1.31	0.7036	0.4293	
Residual	13.06	7	1.87			
Lack of Fit	7.99	3	2.66	2.10	0.2426	not significant

Appendix 12